Quantitative Characterization of Pressure-related Turbulence Transport Terms using Simultaneous Nonintrusive Pressure and Velocity Measurement*

Xiaofeng Liu[1] and Joseph Katz[2]

[1]Department of Aerospace Engineering
San Diego State University
Email: Xiaofeng.Liu@mail.sdsu.edu

[2]Department of Mechanical Engineering
Johns Hopkins University

UMich/NASA Symposium on
Advances in Turbulence Modeling
Ann Arbor, Michigan
July 11-13, 2017

SAN DIEGO STATE UNIVERSITY

*Sponsors: ONR, NSF and SDSU

JOHNS HOPKINS UNIVERSITY

Outline of Presentation

- Background and Motivation:
  - Overview of the Notre Dame Wake Study
- Pressure Reconstruction Methods
- Experimental Setup
- Measurement Results on Pressure-Related Turbulence
  - Pressure-Velocity Correlation
  - Pressure Diffusion Distribution and Comparison with Turbulence Diffusion and Total Production Terms
  - Comparisons of Velocity-Pressure-Gradient, Pressure-Strain and Pressure Diffusion Terms
- Conclusions

ND Wake Study*: High-Lift Wake Flow in Pressure Graidents

<u>Two major features</u> associated with the wake flow generated by upstream elements in a high lift system :

— **The wake development invariably occurs in a <u>strong pressure gradient environment</u>.**

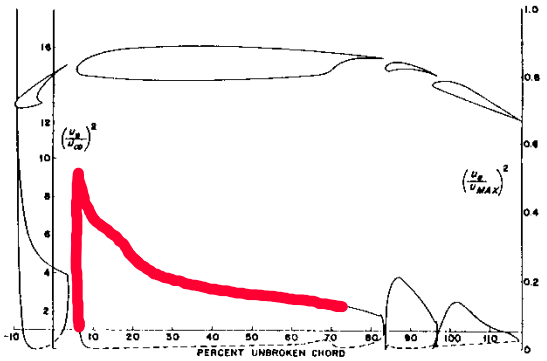

(From A.M.O. Smith, 1975)

— **The wake profile is <u>highly asymmetric</u>.**

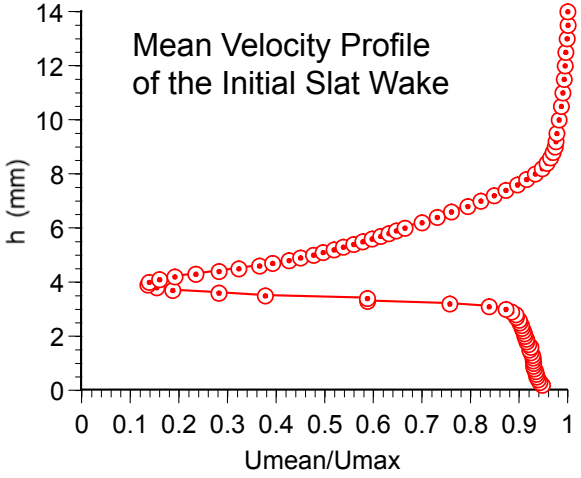

(From Thomas, Nelson and Liu, 1998)

*Sponsor: NASA Langley Research Center (NASA NAGI-1987)
(Thanks to Ben Anders, Christopher Rumsey and John Carlson)

ND Wake Study: Experimental Facility

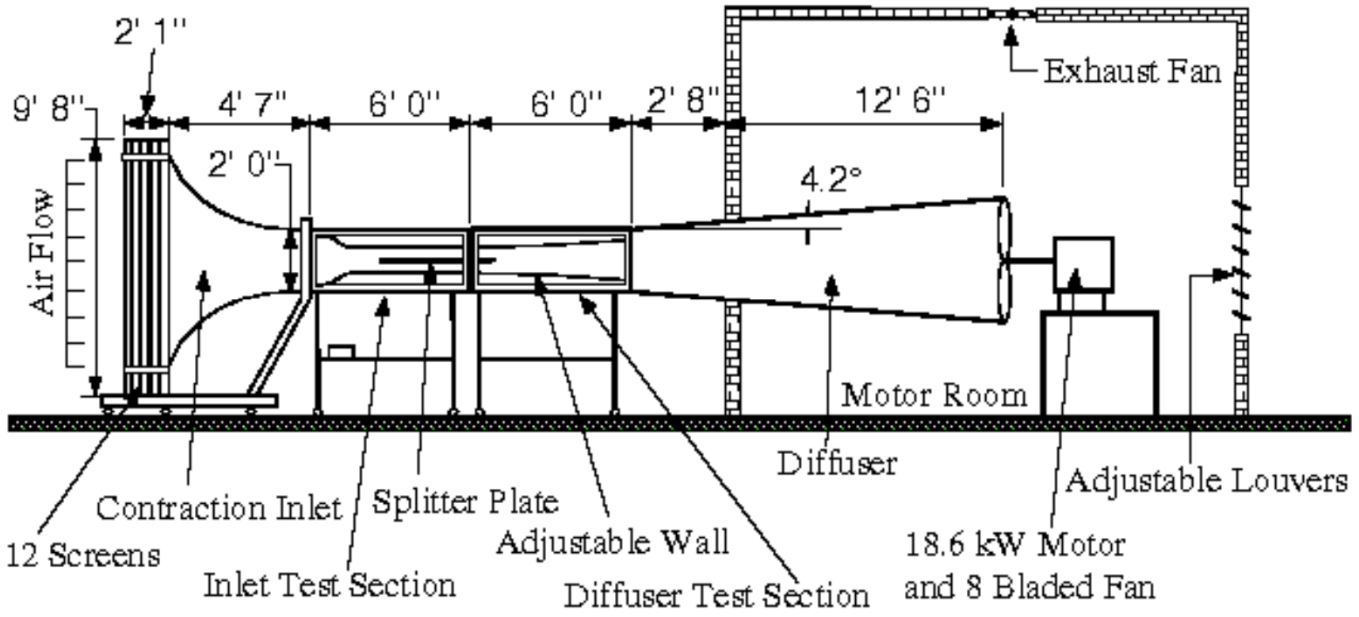

Schematic of Notre Dame Subsonic Wind Tunnel for the Wake Study

- Contraction ratio of inlet
  20.25:1
- Speed of wind tunnel
  ~ 30 m/s
- Reynolds number (based on c)
  $Re \approx 2.4 \times 10^6$
- Dimension of test section
  2 ft.(width) × 2 ft.(height) × 12 ft. (length)
- Chord of the splitter plate
  c = 48 in ≈1.22m
- Instrumentation for Flow Survey
  X-wire and **LDV**

Reynolds number based on the initial wake momentum thickness **$Re_\theta = 1.5 \times 10^4$.**

Wake Structure Nomenclature

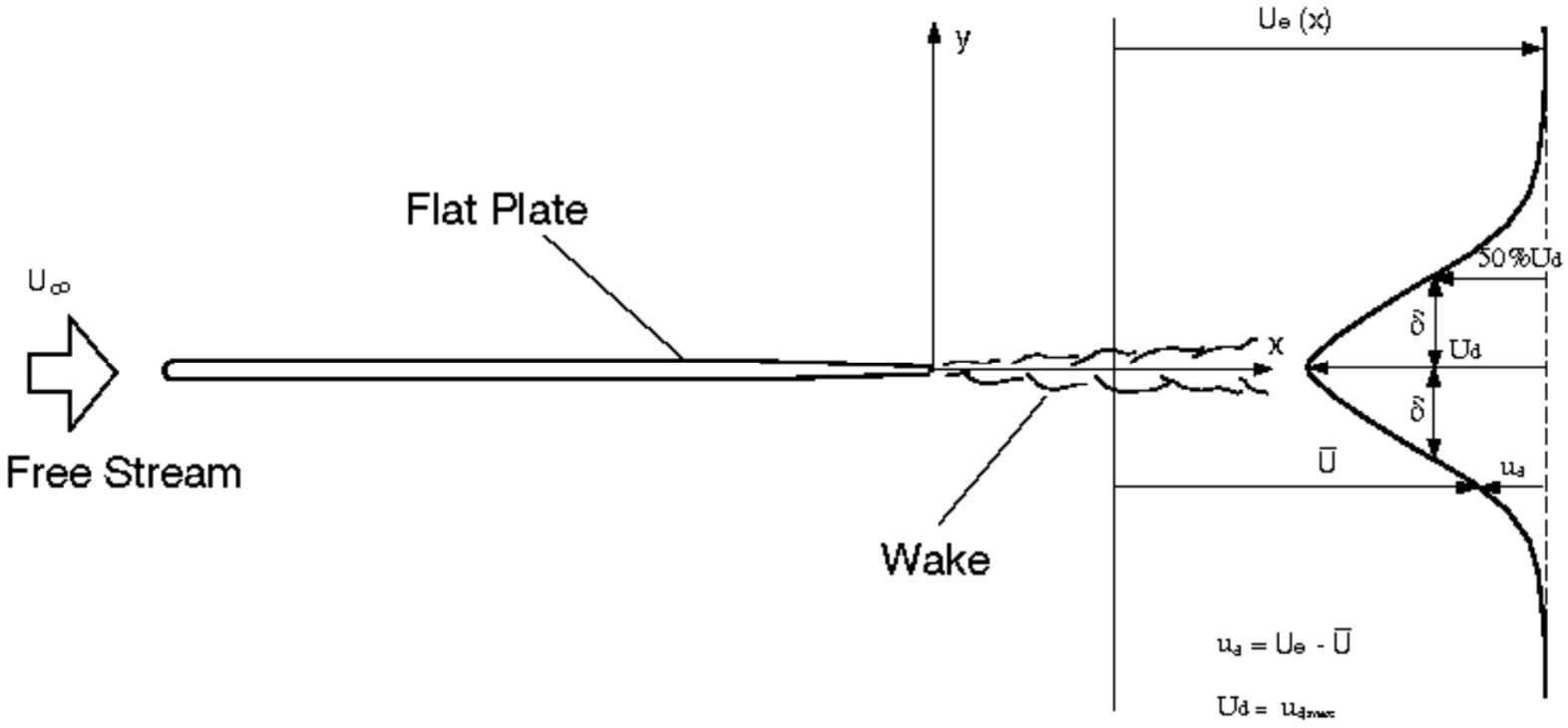

ND Wake Study: Constant Pressure Gradient Environment

One Unique Feature: The imposed pressure gradient is **constant** in the flow field .

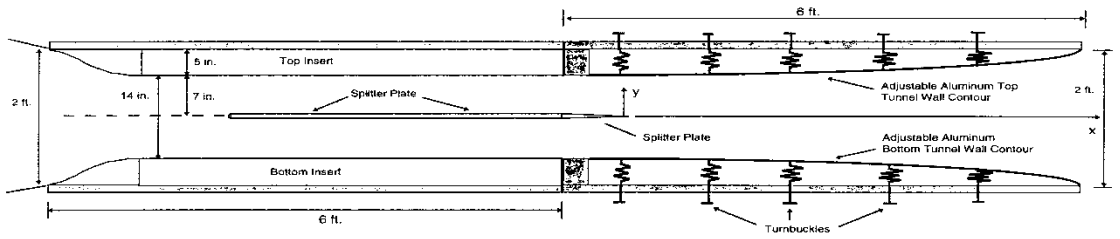

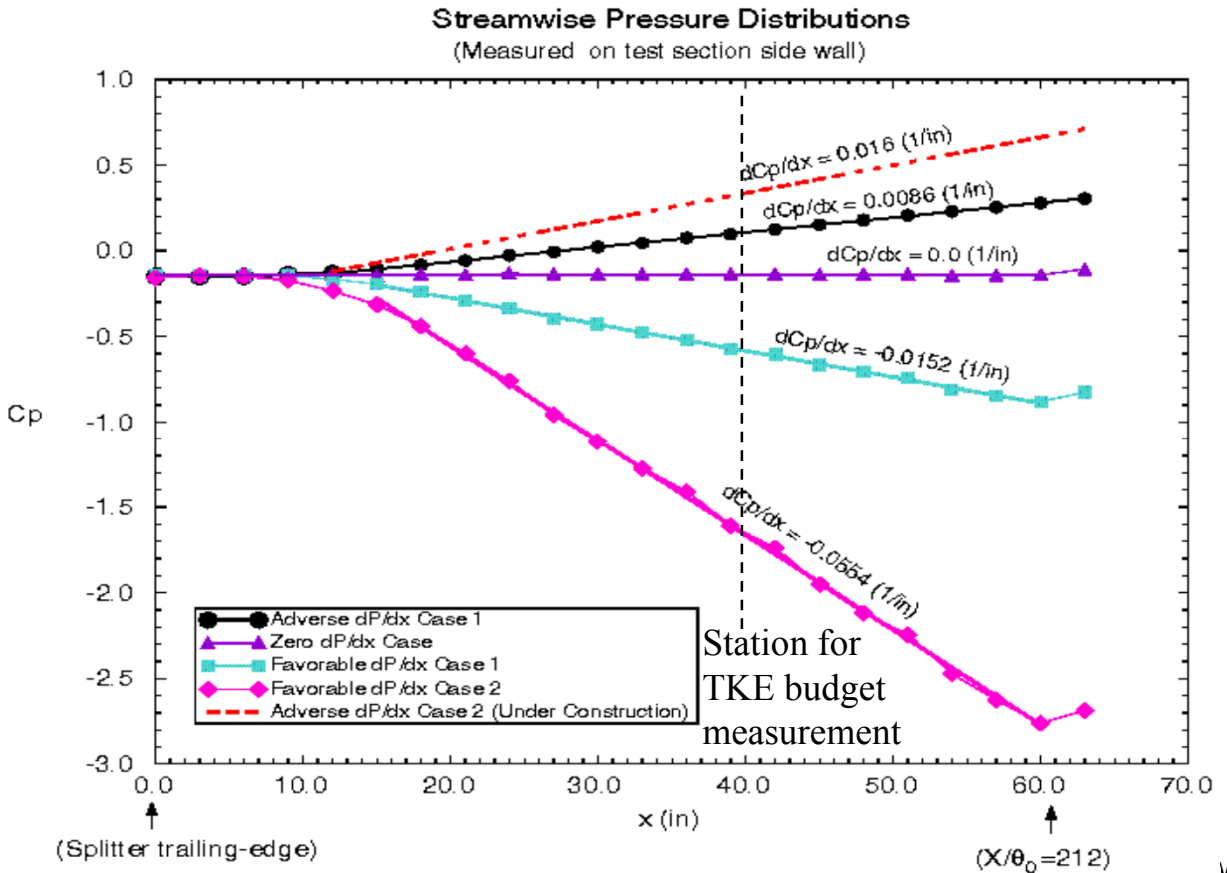

Station for TKE budget measurement

wake;
152 for asymmetric wake

Expansion of the Turbulent Kinetic Energy Equation

For **steady, 2-D in the mean, incompressible, homogeneous turbulence** flow, we have $\frac{\partial}{\partial t}(\overline{\ }) = 0$, $\overline{U_3} = 0$ and $\frac{\partial}{\partial x_3}(\overline{\ }) = 0$. Also we have, from continuity equation, $\frac{\partial \overline{U_2}}{\partial x_2} = -\frac{\partial \overline{U_1}}{\partial x_1}$. Thus, the turbulent kinetic energy equation can be **<u>simplified</u>** as follows:

$$\underbrace{\overline{U_1}\frac{\partial}{\partial x_1}\left(\frac{\overline{q^2}}{2}\right) + \overline{U_2}\frac{\partial}{\partial x_2}\left(\frac{\overline{q^2}}{2}\right) =}_{\text{Convection}}$$

No device is capable of measuring this term to date.

$$\underbrace{-\frac{\partial}{\partial x_1}\overline{u_1'\frac{p'}{\rho}} - \frac{\partial}{\partial x_2}\overline{u_2'\frac{p'}{\rho}}}_{\text{Pressure Diffusion}} \quad \underbrace{-\frac{\partial}{\partial x_1}\overline{\frac{1}{2}\left(u_1'^3 + u_1'u_2'^2 + u_1'u_3'^2\right)} - \frac{\partial}{\partial x_2}\overline{\frac{1}{2}\left(u_1'^2u_2' + u_2'^3 + u_2'u_3'^2\right)}}_{\text{Turbulence Diffusion}}$$

Assume $\overline{u_2'u_3'^2} \approx \overline{u_3'^3}$

This term requires miniature probes to capture the finest eddy of motion

$$\underbrace{-\left(\overline{u_1'^2} - \overline{u_2'^2}\right)\frac{\partial \overline{U_1}}{\partial x_1} - \overline{u_1'u_2'}\left(\frac{\partial \overline{U_1}}{\partial x_2} + \frac{\partial \overline{U_2}}{\partial x_1}\right)}_{\text{Production}} \quad \underbrace{+\frac{\nu}{2}\frac{\partial^2 \overline{q^2}}{\partial x_1^2} + \frac{\nu}{2}\frac{\partial^2 \overline{q^2}}{\partial x_2^2}}_{\text{Viscous Diffusion}}$$

This term is negligible.

$$\underbrace{-\nu\left(\overline{\left(\frac{\partial u_1'}{\partial x_1}\right)^2} + \overline{\left(\frac{\partial u_1'}{\partial x_2}\right)^2} + \overline{\left(\frac{\partial u_1'}{\partial x_3}\right)^2} + \overline{\left(\frac{\partial u_2'}{\partial x_1}\right)^2} + \overline{\left(\frac{\partial u_2'}{\partial x_2}\right)^2} + \overline{\left(\frac{\partial u_2'}{\partial x_3}\right)^2} + \overline{\left(\frac{\partial u_3'}{\partial x_1}\right)^2} + \overline{\left(\frac{\partial u_3'}{\partial x_2}\right)^2} + \overline{\left(\frac{\partial u_3'}{\partial x_3}\right)^2}\right)}_{\text{Dissipation}} \qquad (3)$$

Sensors for the TKE Budget Measurements

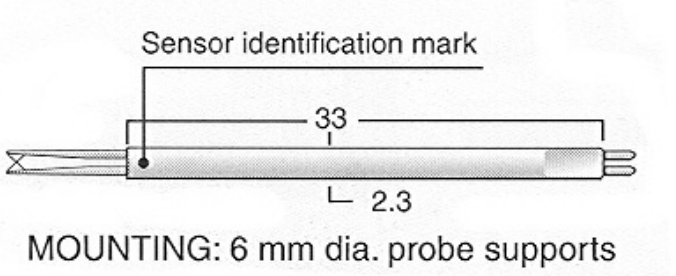

X-wire Probe
(Adapted from Dentec Catalog)

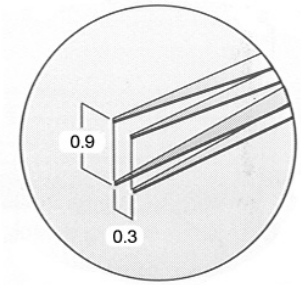

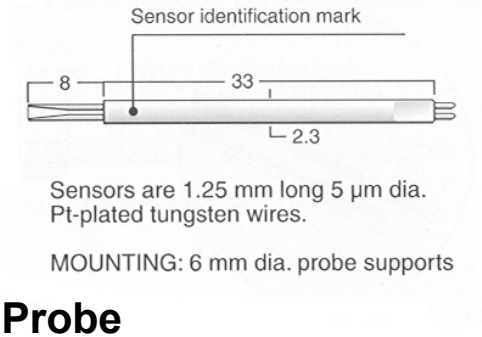

Parallel Probe
(Adapted from Dentec Catalog)

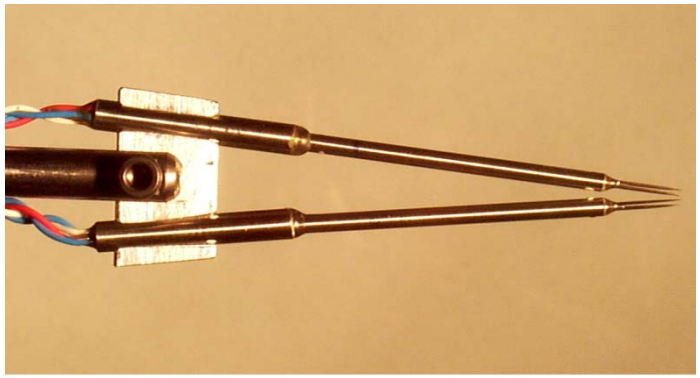

Twin X-wire Configuration

- Constant Temperature Hot-wire Anemometer
  - IFA-100 anemometer.
- X-wire Probe
  - Auspex type AHWX-100, tungsten wire, diameter 5µm, length 1.2mm.
- Parallel Probe
  - Auspex type AHWG-100, tungsten wire, diameter 5µm, length 0.9mm, spacing between dual sensors 0.3mm.
- Twin X-wire Configuration
  - Two identical X-wire probes of Auspex type AHWX-100.
- Cut-off Frequency of Low Pass Filter
  - 20 kHz
- Sampling Frequency
  - 40 kHz (Nyquist Frequency = 20 kHz)
- Total record length per sample
  - 13.1 sec.
- Kolmogorov microscales of wake flow
  - $L_K = (\nu^3/\varepsilon)^{1/4} \approx 0.1$ mm; $T_K = (\nu/\varepsilon)^{1/2} \approx 0.4$ ms.

ND Wake Study: TKE Budget for the Symmetric Wake in ZPG

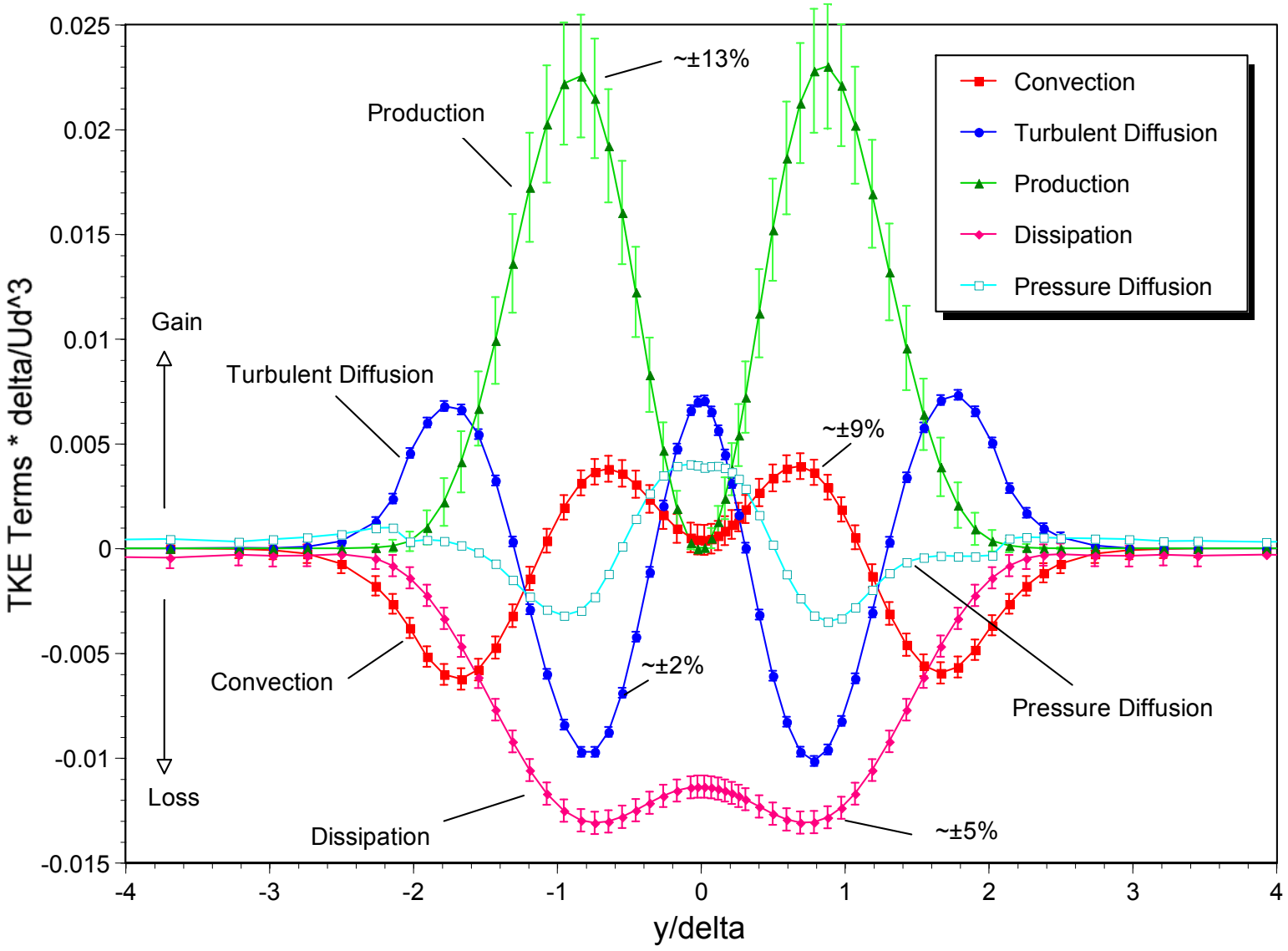

(0 = Convection + Production + Turbulent Diffusion + Pressure Diffusion + Dissipation)

ND Wake Study: Comparison of TKE Budget for the Symmetric Wake in ZPG with DNS Result (Moser, Rogers & Ewing, 1998)

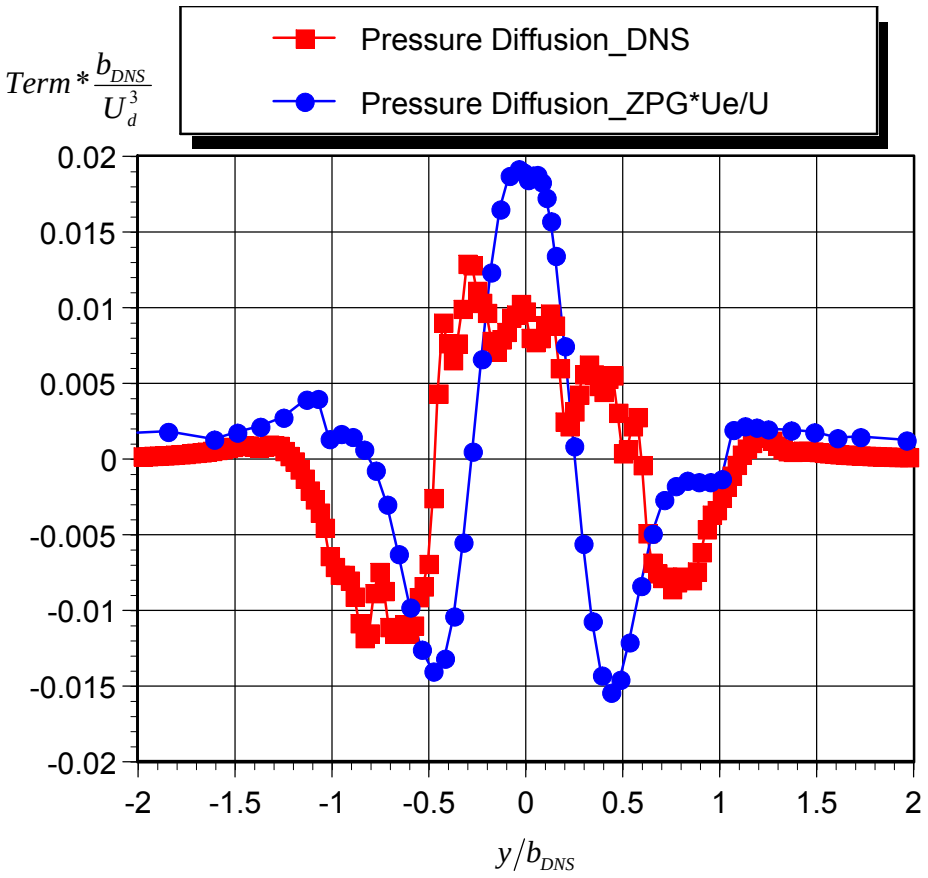

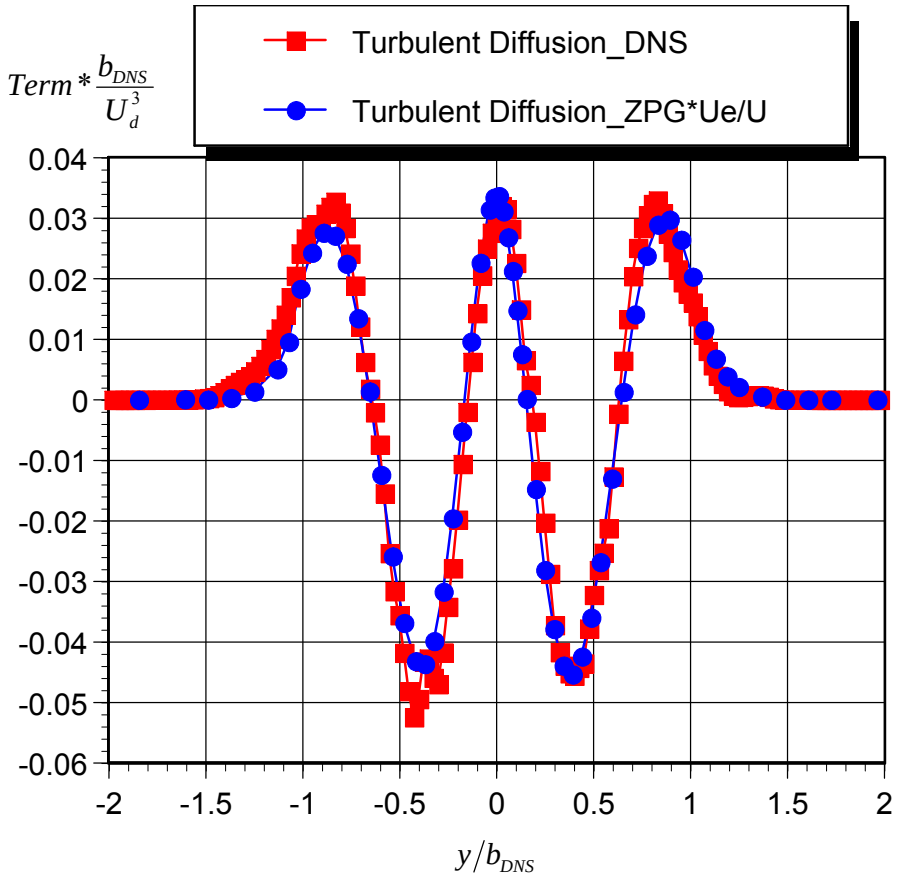

Note the difference between the DNS and the experimental data:
DNS result is based on data obtained in the similarity region;
Our experimental result is in the near wake region with $x/\theta = 141$

(The DNS Data Courtesy of Michael M. Rogers)

ND Wake Study: Comparison of TKE Budget for the Symmetric Wake in ZPG with DNS Result (Moser, Rogers & Ewing, 1998)

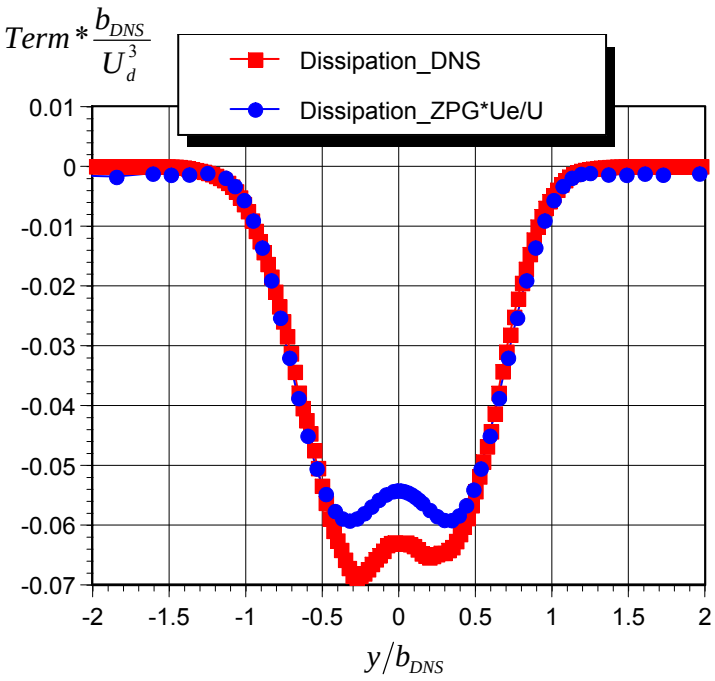

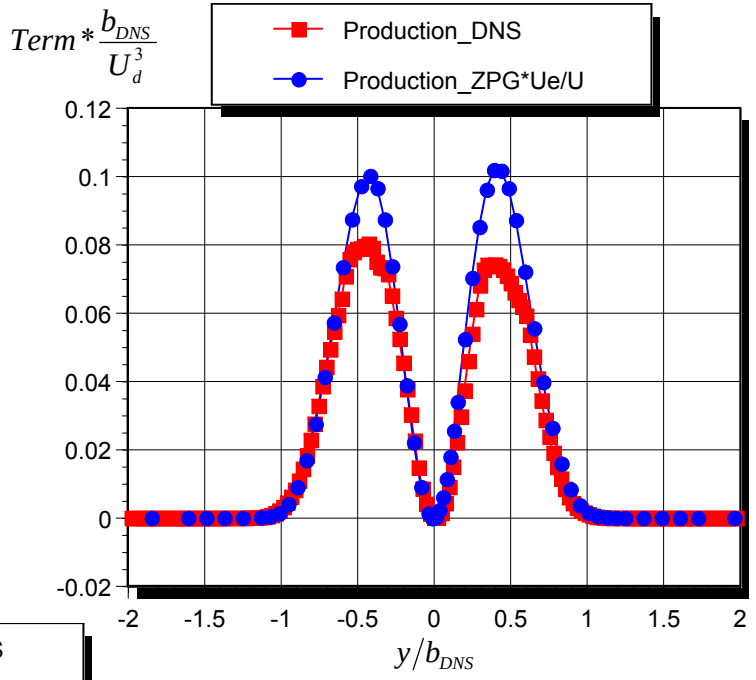

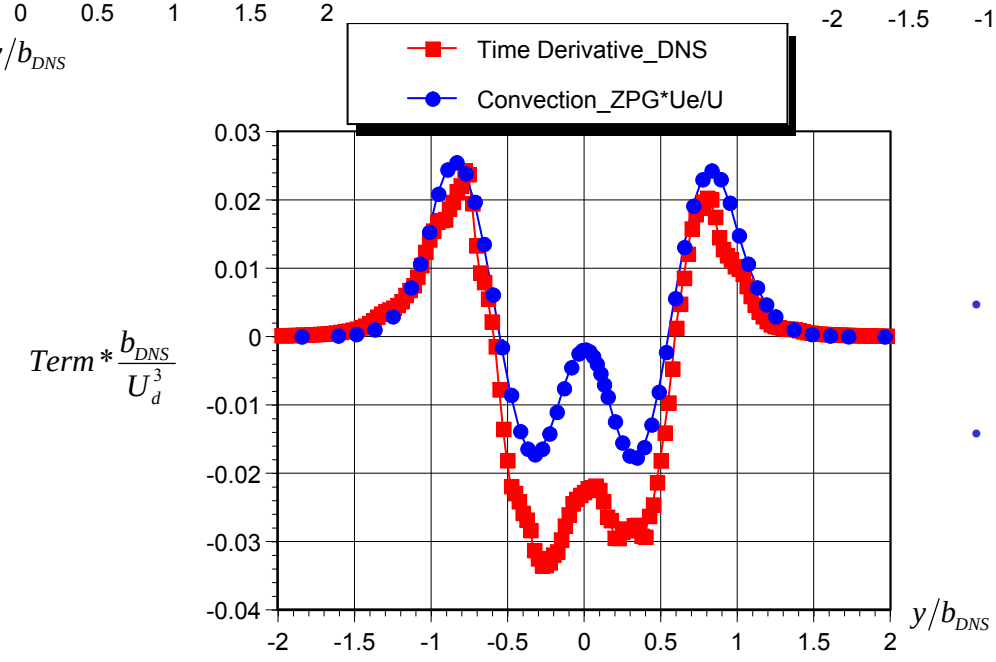

- The DNS Data Courtesy of Michael M. Rogers.
- Results published in Experiments in Fluids (Liu and Thomas, 2004)

Reynolds Stress Transport Equation

$$\underbrace{\frac{D}{Dt}\left(\overline{u_i'u_j'}\right)}_{\text{Material derivative of Reynolds stress (unsteady term + convection)}} = \underbrace{-\frac{\partial}{\partial x_i}\overline{u_i'u_j'u_k'}}_{\text{turbulence diffusion}} + \underbrace{\frac{\partial}{\partial x_k}\left(\nu\frac{\partial}{\partial x_k}\overline{u_i'u_j'}\right)}_{\text{viscous diffusion}} + \underbrace{P_{ij}}_{\text{production}} + \underbrace{\Pi_{ij}}_{\text{velocity-pressure-gradient}} - \underbrace{\varepsilon_{ij}}_{\text{dissipation}}$$

where

$$P_{ij} = -\overline{u_i'u_k'}\frac{\partial \overline{U}_j}{\partial x_k} - \overline{u_j'u_k'}\frac{\partial \overline{U}_i}{\partial x_k} \qquad \varepsilon_{ij} = 2\nu\overline{\left(\frac{\partial u_i'}{\partial x_k}\frac{\partial u_j'}{\partial x_k}\right)}$$

$$\Pi_{ij} = \underbrace{-\frac{1}{\rho}\overline{\left(u_i'\frac{\partial p'}{\partial x_j} + u_j'\frac{\partial p'}{\partial x_i}\right)}}_{\text{velocity-pressure-gradient}} = \underbrace{-\left(\frac{\partial}{\partial x_i}\frac{\overline{u_j'p'}}{\rho} + \frac{\partial}{\partial x_j}\frac{\overline{u_i'p'}}{\rho}\right)}_{\text{pressure diffusion, } D_{ij}^{(p)}} + \underbrace{\overline{\frac{p'}{\rho}\left(\frac{\partial u_i'}{\partial x_j} + \frac{\partial u_j'}{\partial x_i}\right)}}_{\text{pressure-strain, } R_{ij}}$$

i.e., $\Pi_{ij} = D_{ij}^{(p)} + R_{ij}$

Note: *Pressure diffusion* is also called *the gradient of the Reynolds stress flux due to fluctuating pressure*.

Importance of Measurement of Pressure-Strain Terms

- **Importance of intercomponent energy transfer**

$$R_{11} + R_{22} + R_{33} = 0$$

Because for incompressible flow $\overline{\frac{2p'}{\rho}\left(\frac{\partial u_1'}{\partial x_1} + \frac{\partial u_2'}{\partial x_2} + \frac{\partial u_3'}{\partial x_3}\right)} = 0$

  - **Pressure-strain terms** are responsible for **redistribution of energy among components of the turbulence normal stresses**, i.e., intercomponent energy transfer among fluctuating components.

  - Thus pressure-strain terms serve as the primary mechanism for the return-to-isotropy process (Pope, 2000) of the anisotropic turbulence.

  - Pressure-strain terms play a major role in defining turbulence development.

  - However, two equation models like k-epsilon make no attempt to differentiate between the three fluctuating velocity components.

  - **Quantifying the intercomponent energy transfer is a key to understanding the physics of turbulent shear flow**.

The State-of-the-Art of the Non-intrusive Pressure Measurement Techniques

- The **instantaneous spatial pressure distribution** in an incompressible turbulent flow field can be measured non-intrusively by integration of the measured material acceleration, which is the dominant contributor to pressure gradient for flow at high Reynolds number:

$$\nabla p = -\rho\left(\underbrace{\frac{D\vec{U}}{Dt}}_{\text{Dominant term}} - \underbrace{\nu\nabla^2\vec{U}}_{\text{Negligible for high Re flow and in regions away from the wall}}\right)$$

- Representative work for the **direct line integration** approach includes Liu and Katz, (**omni-directional integration**, ***2006, Exp. Fluids***; *2008, Phys. Fluids;* ***2013 JFM***); Joshi, Liu and Katz (*2014 JFM*); **Liu *et al.* (AIAA Paper 2016-1049)** etc.
- In addition, the pressure distribution can also be obtained by **solving the Poisson equation**, as shown in Violato *et al.* (*2008*, *Exp. Fluids*) , and de Kat and van Oudheusden (*2012*, *Exp. Fluids*), etc.
- The robustness of the omni-directional integration method has been confirmed by Charonko *et al*. (2010).
- **Least Square Reconstruction** (e.g., Jeon *et al.*, 2015), or **Direct Matrix Inversion** (Liu and Katz 2006), **POD-based Irrotation Correction** (Wang *et al.*, 2016).
- **Poisson equation** ← math equivalent → **Least Square Reconstruction** (Wang *et al.*, 2017).

Circular Virtual Boundary Omni-Directional Integration (Liu and Katz, 2006, 2008, 2013)

– Circular Virtual Boundary Omni-Directional Integration over the entire flow field to obtain the instantaneous spatial pressure distribution:

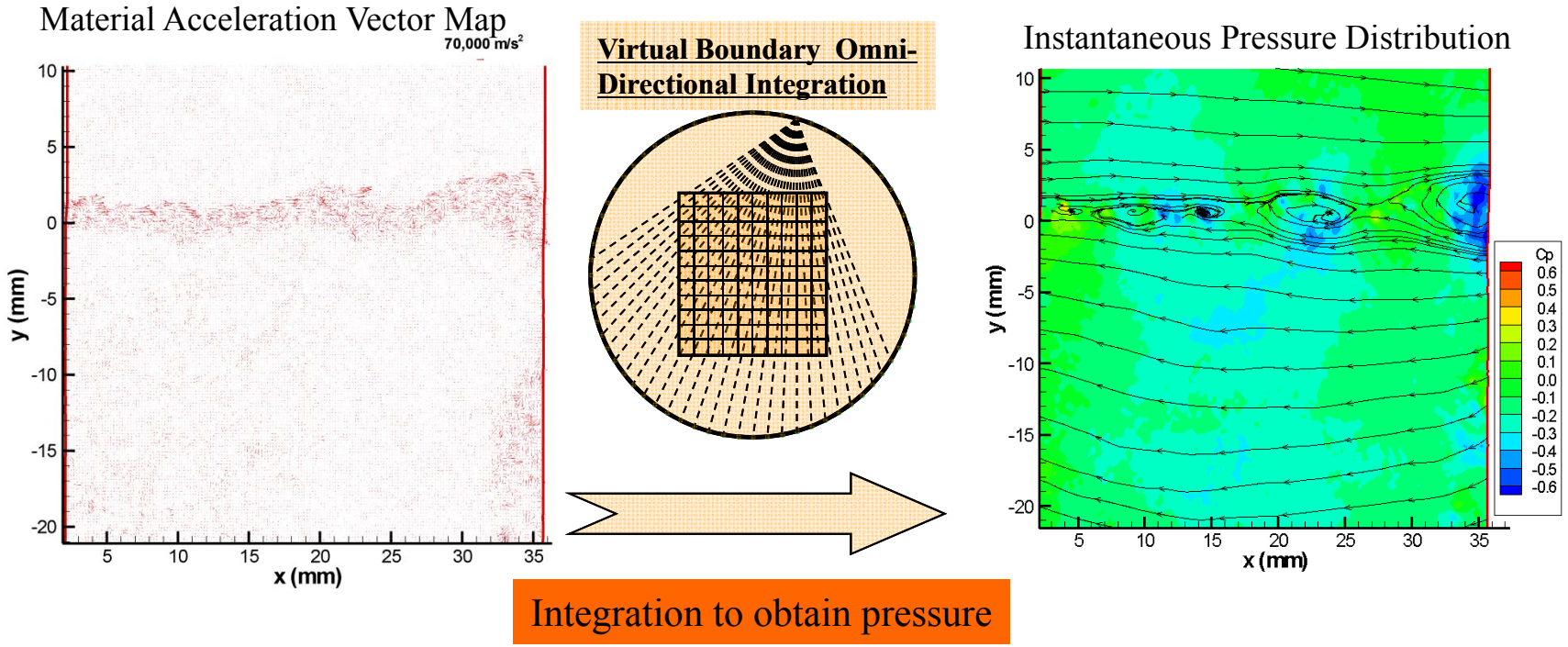

Google key word: **Pressure PIV**

Liu and Katz 2013, Journal of Fluid Mechanics, vol. 728, pp. 417-457.
Liu and Katz 2008, Physics of Fluids, 20, 041702.
Liu and Katz 2006, Experiments in Fluids, 41, 227-240.

Rotating Parallel Ray Omni-Directional Integration

Old Algorithm (2007, 2008)
Circular virtual boundary omni-directional integration algorithm.

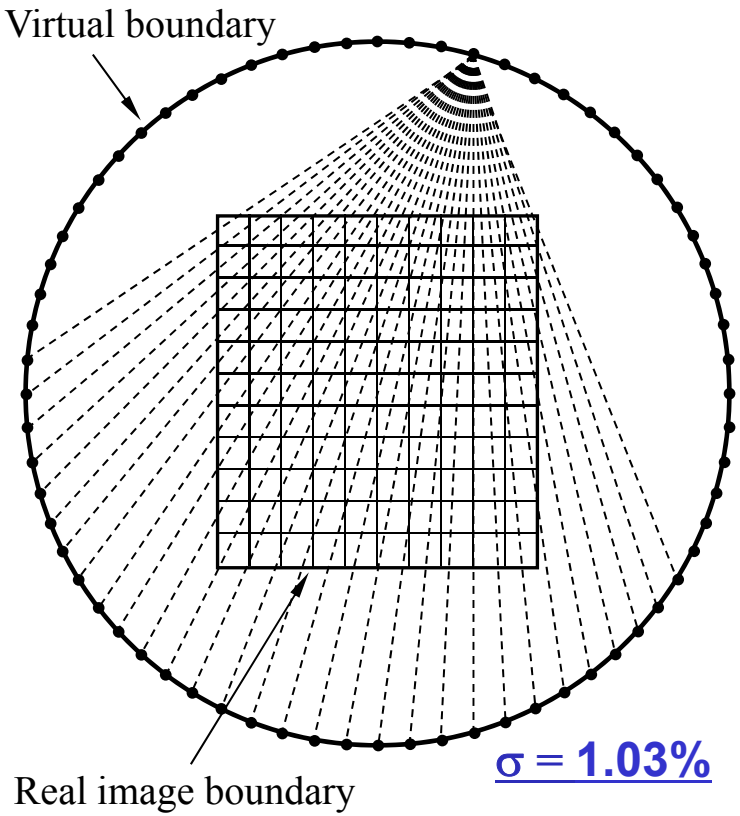

σ = 1.03%

New Algorithm (Liu *et al.* AIAA Paper 2016-1049)
Rotating parallel ray omni-directional integration algorithm.

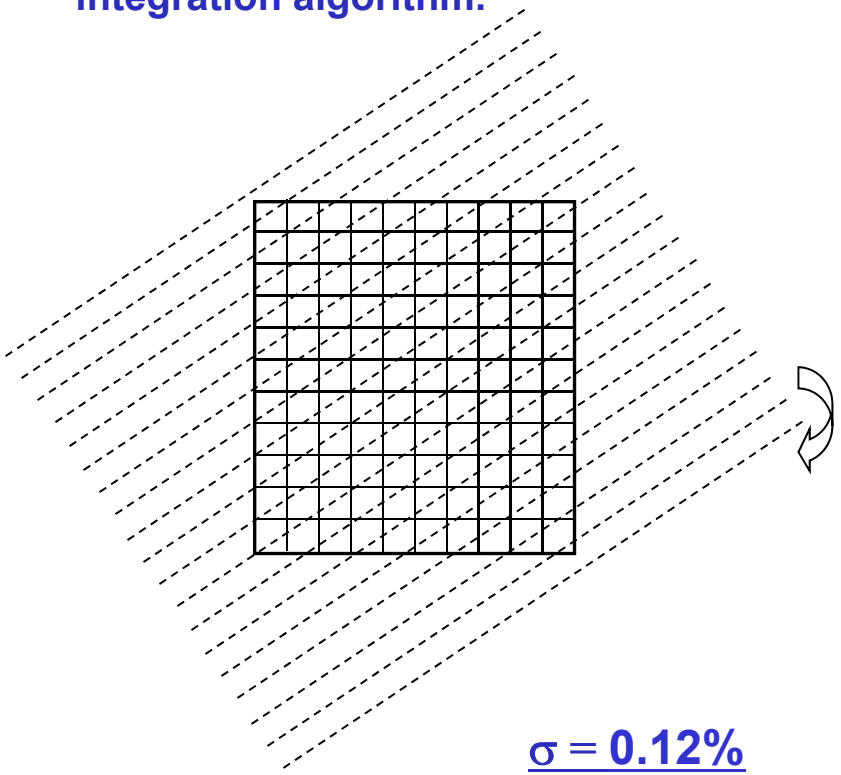

σ = 0.12%

- An inherent defect in the old algorithm: Location dependence of integration weight. Other than the points near the geometric center, points at other places do not see a uniform weight of contribution from all directions.
- **New algorithm: Equal Weights of integration involvement can be generated, thus eliminates the defect in location dependence**.

Time-Resolved PIV Measurements

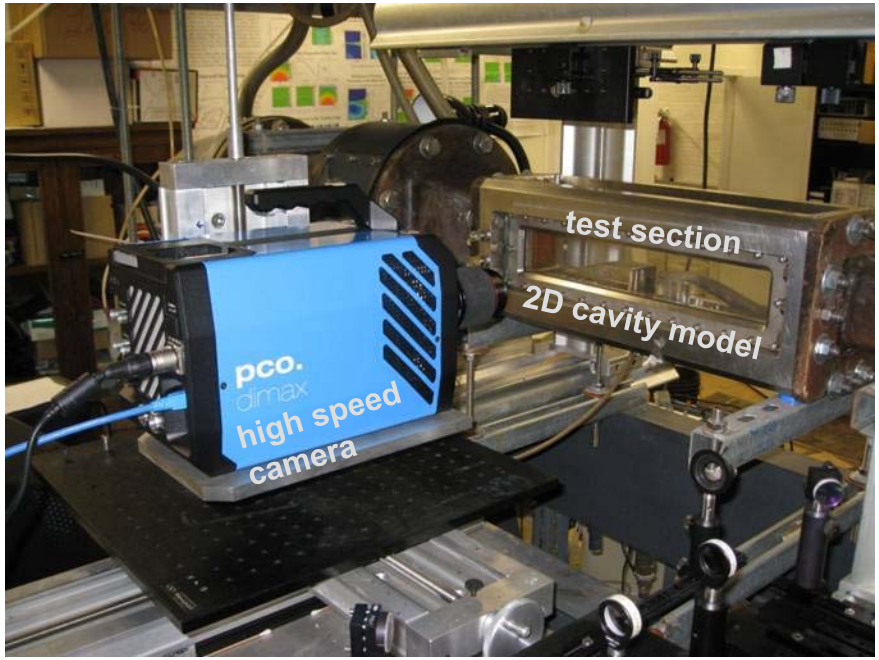

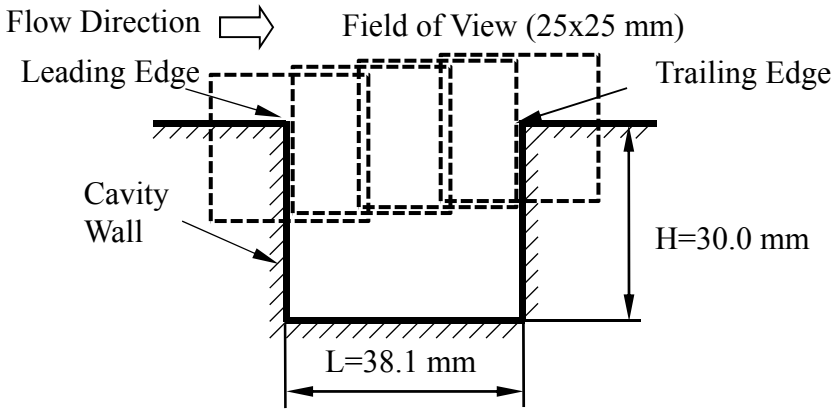

- High Speed Camera
  - PCO.dimax, 12 bit
  - Resolution: 1008x1000 pixels @ 4500 fps
- High Repetition Rate Laser
  - Photonics DM60-527 Nd:YLF
  - Maximum pulse rate - 10 kHz
  - Pulse energy: 60mJ at 1KHz
- Tracer Particles
  - -- Hollow glass spheres, 8-12μm
- Dimensions of Cavity
  - Cavity width (L): 38.1mm
  - Cavity depth (H): 30.0mm
- Free Stream Speed in Experiment
  - 1.2m/s
- Reynolds Number
  - Re=40,000 (based on cavity width)
  - Re_θ=316, boundary layer turbulent
- Image size: 25x25 mm
- Vector Spacing: 0.2 mm
- Interrogation window size: 0.4x0.4 mm

Incoming Turbulent Boundary Layer Profile

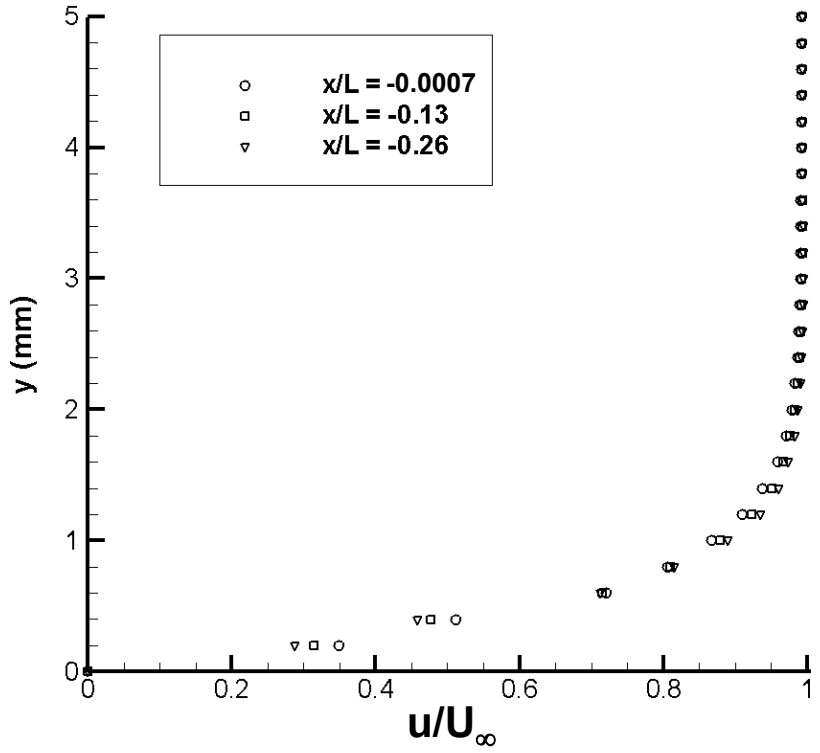

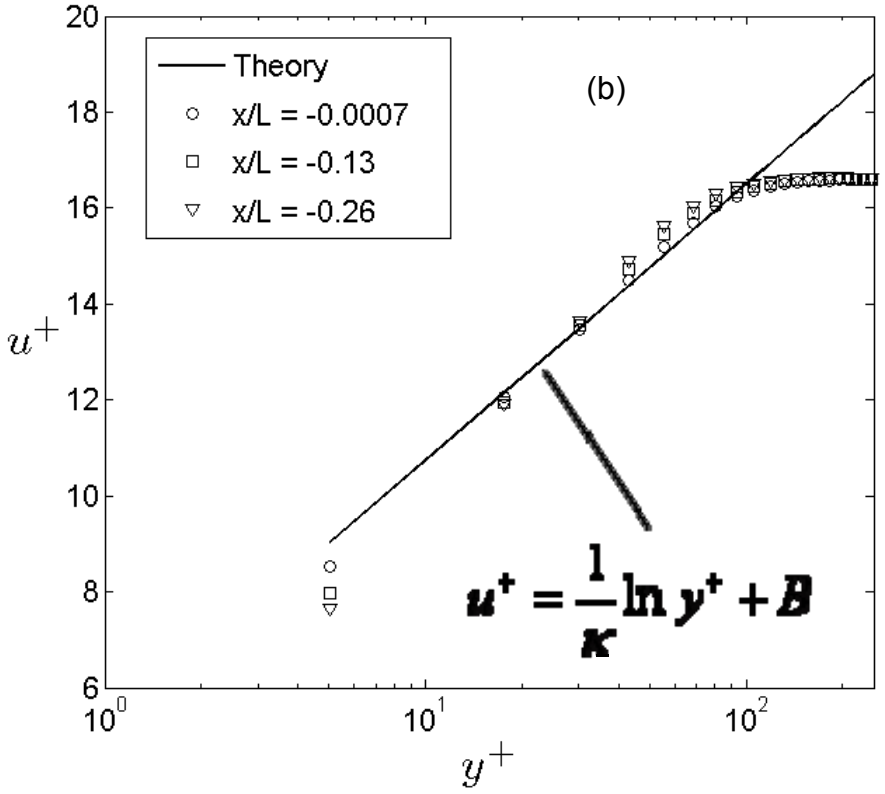

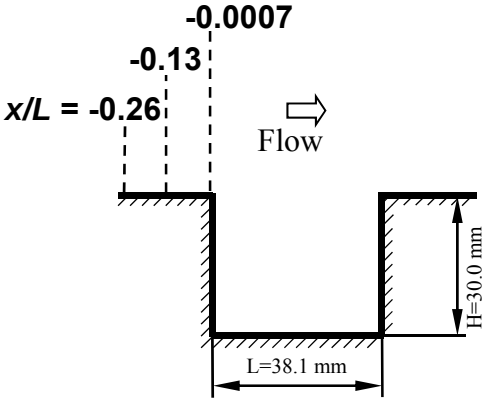

Location x/L	Displacement thickness δ* (mm)	Momentum thickness θ (mm)	Shape factor H (= δ*/ θ)	Skin friction coefficient C_f	Friction velocity u_τ (m/s)
-0.0007	**0.55**	**0.30**	**1.8**	**0.00715**	**0.0717**
-0.13	0.53	0.27	2.0	0.00715	0.0717
-0.26	0.52	0.25	2.1	0.00715	0.0717

- Recall: for Blasius profile, H ≈ 2.6
  for Klebanoff profile, H≈1.3

$$Re_\theta = 316.$$

Conclusion: The incoming boundary layer is turbulent.

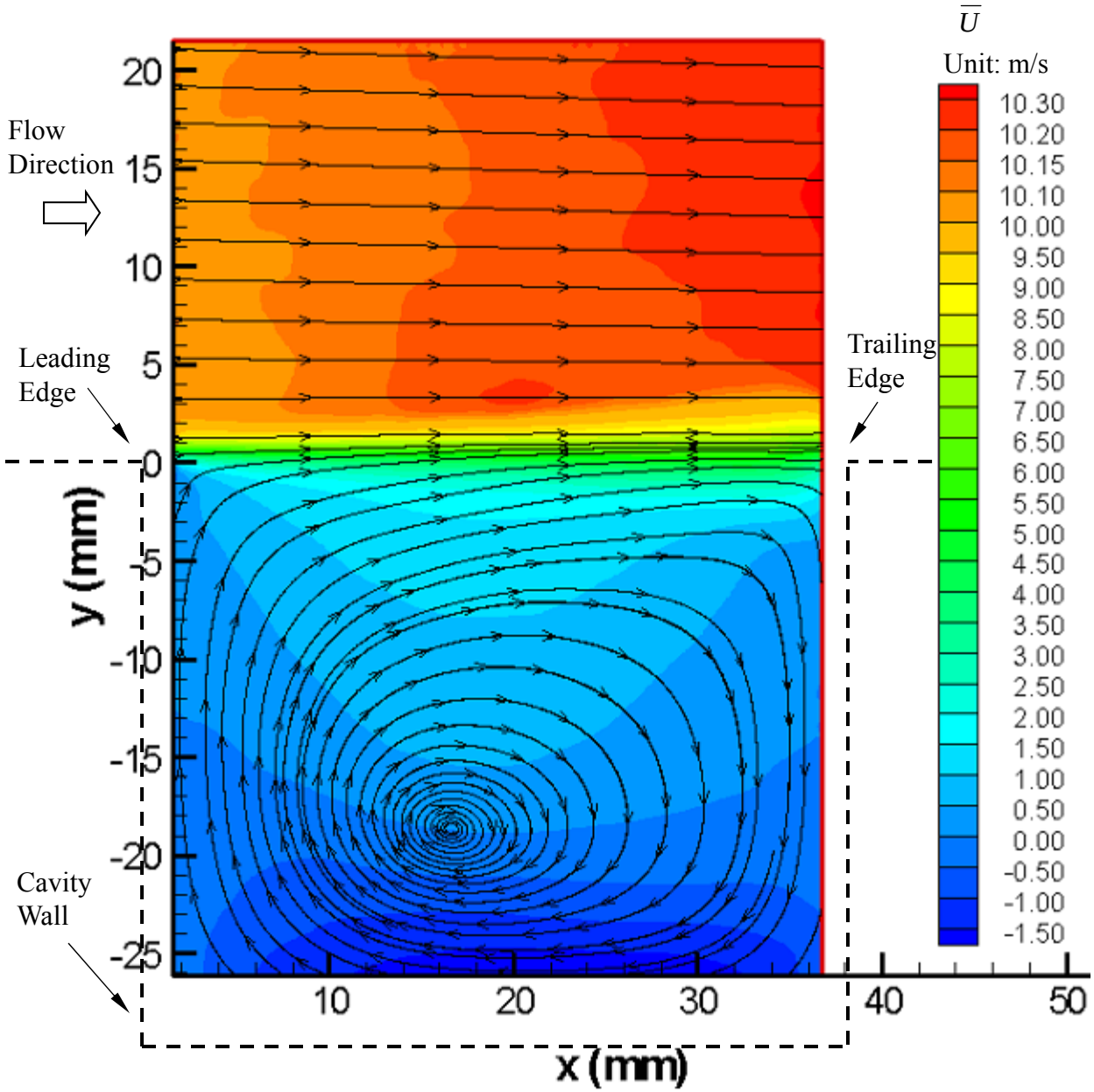

Note: the step of the scale below 10 m/s is 0.5m/s; above 10m/s, the scale is not linear

Instantaneous Pressure Map: Sample 1

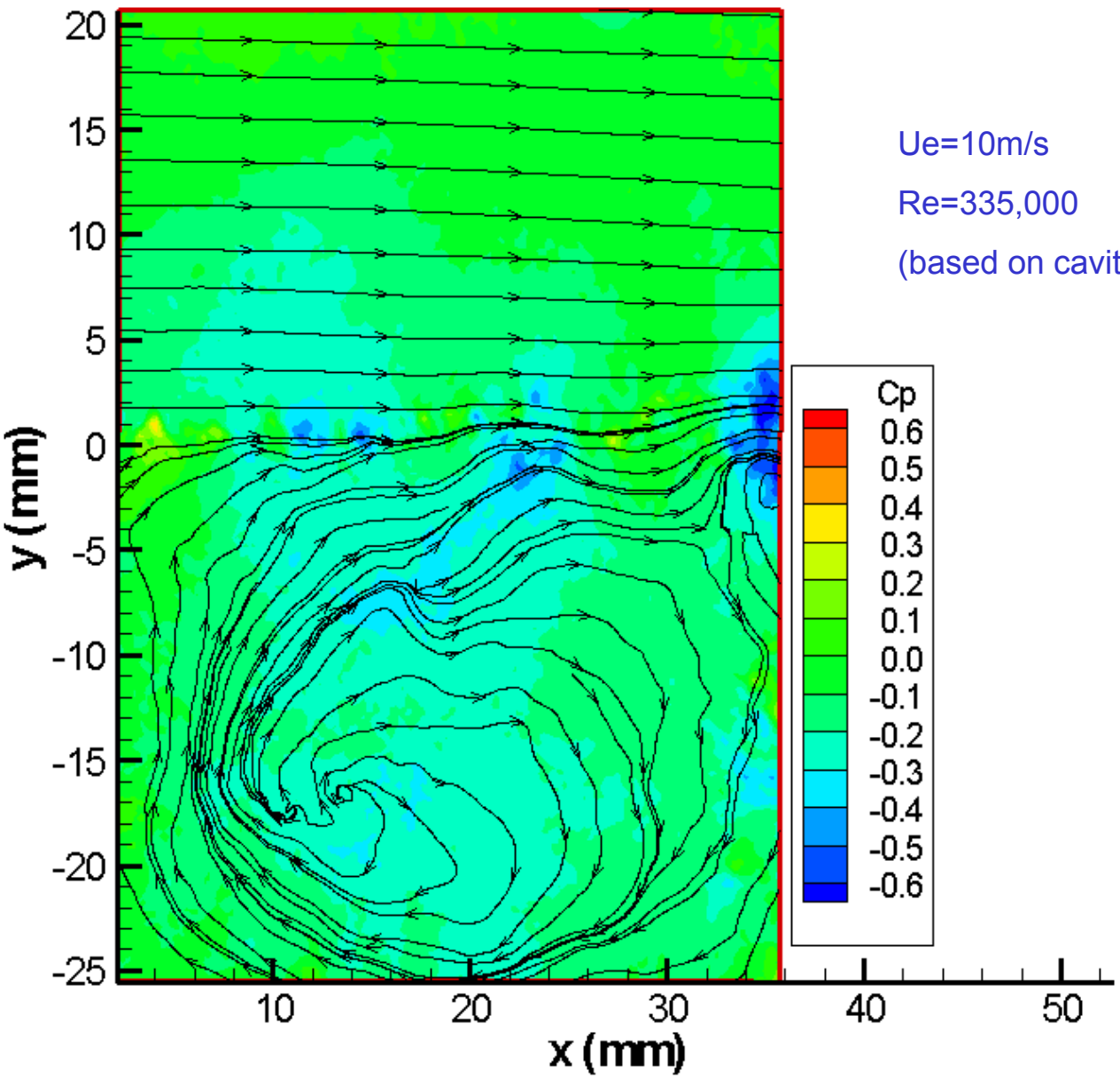

Ue=10m/s

Re=335,000

(based on cavity width)

Instantaneous Pressure Map: Sample 1

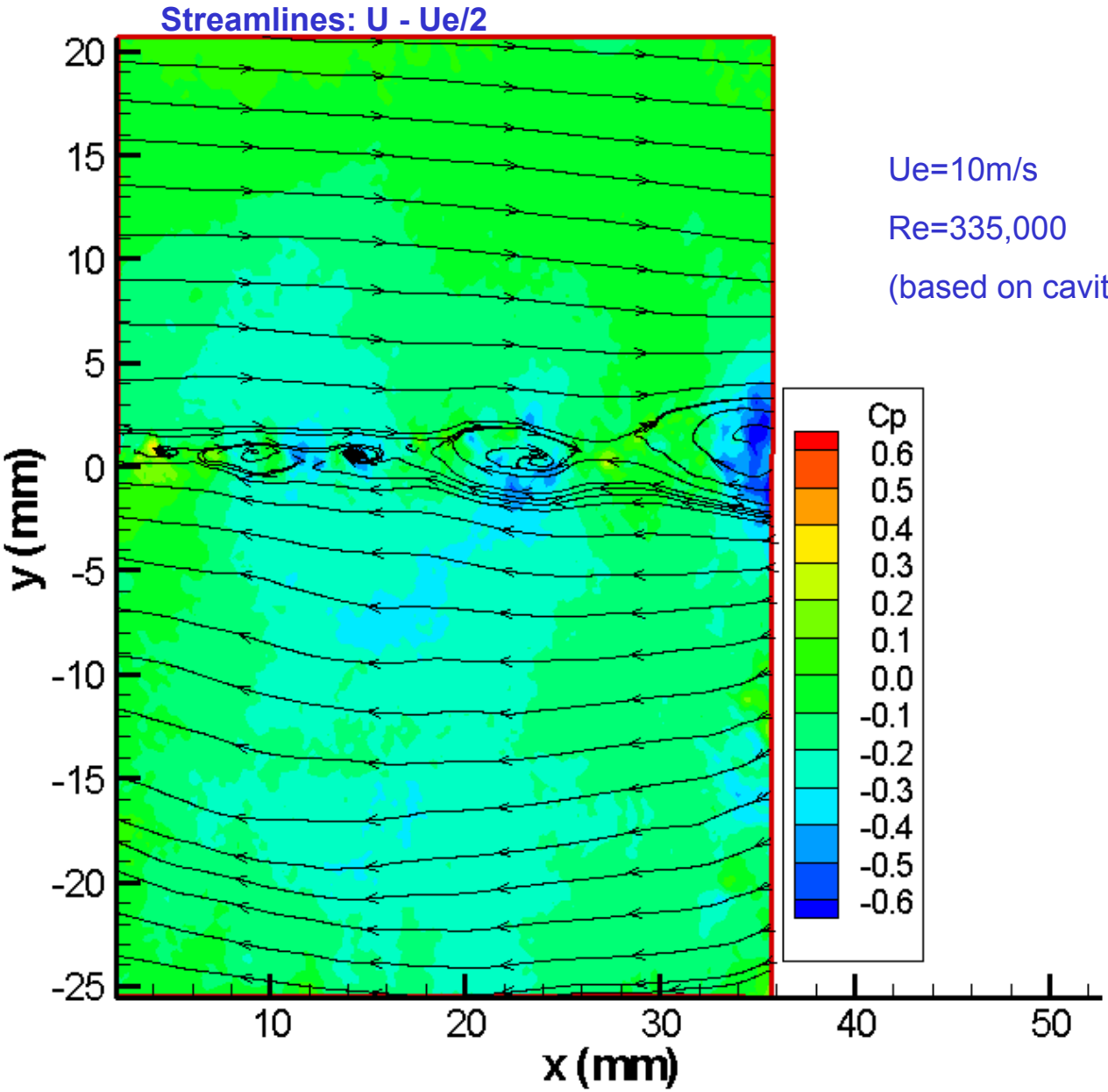

Ue=10m/s

Re=335,000

(based on cavity width)

Sample Raw Data: Characteristic Flow Phenomena
Vortex Shearing and Appearance/ Disappearance

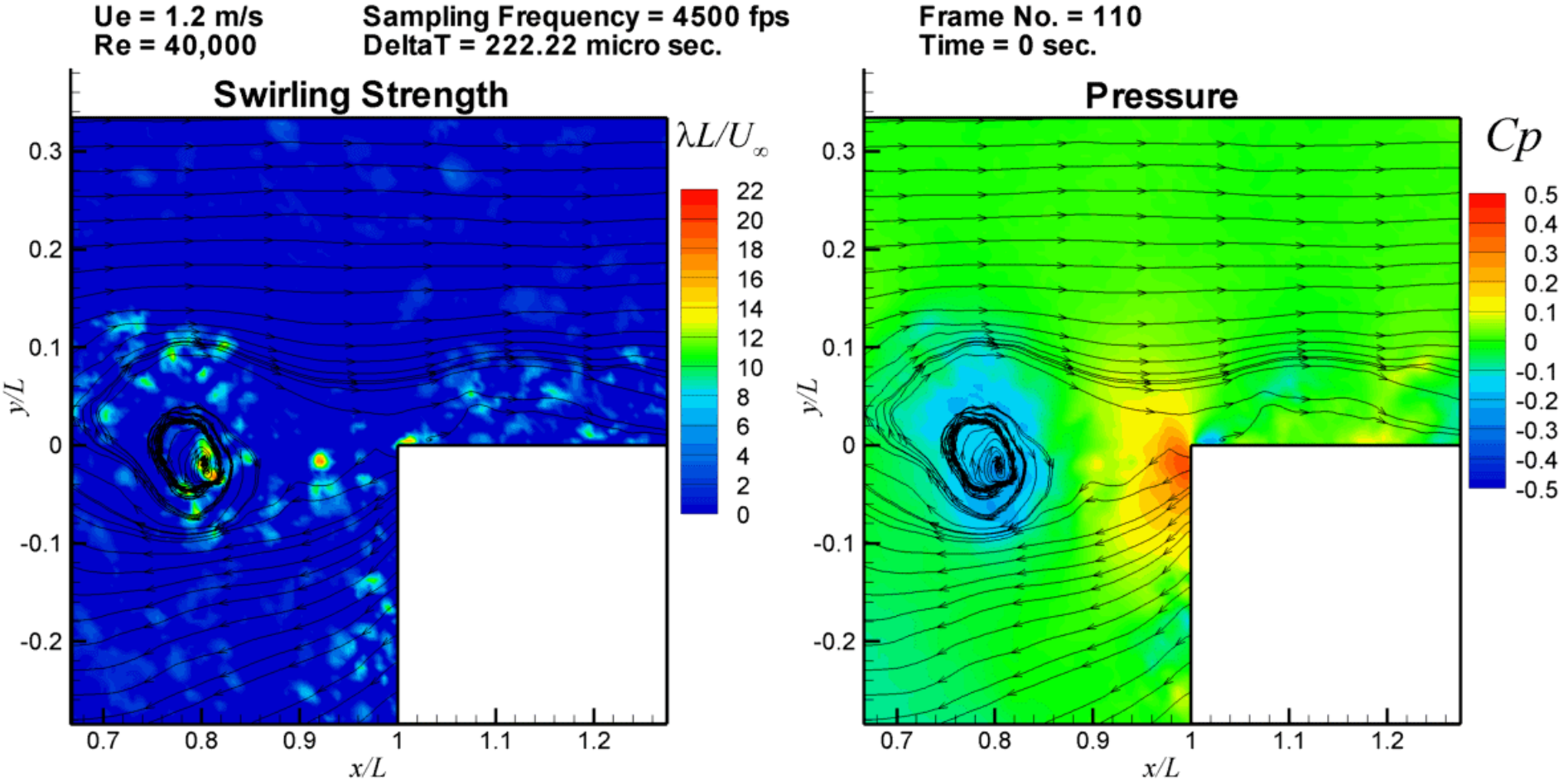

Swirling Strength λ_{ci}

λ_{ci}, the **<u>imaginary part of the complex eigenvalue of the local velocity gradient tensor</u>**, represents the strength of local swirling motion and can be used to identify vortices. (Zhou, *et al* 1996).

Pressure Coefficient C_p

Streamline:

$u - u_c$, assuminging u_c as $0.5U_\infty$

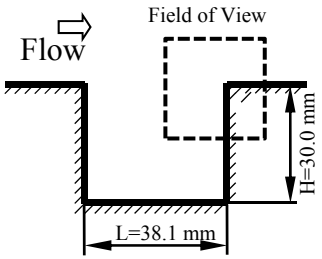

Mean Velocity and Pressure (Ue=1.2 m/s)

Based on an average of 10,000 realizations

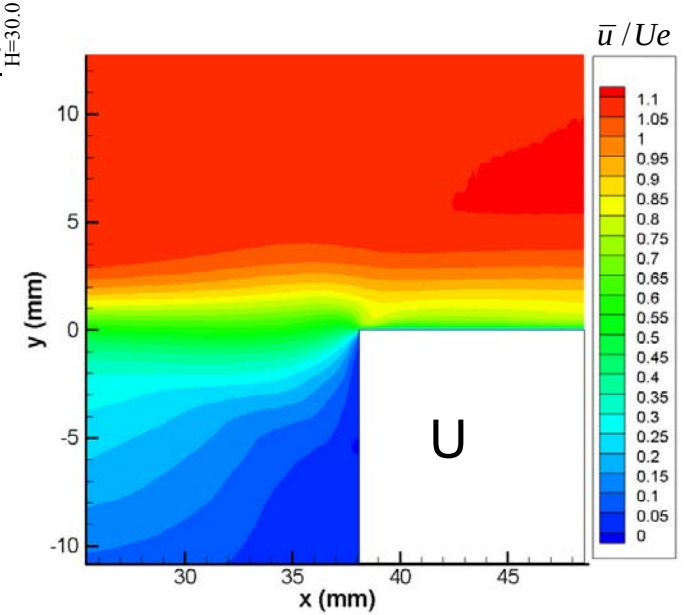

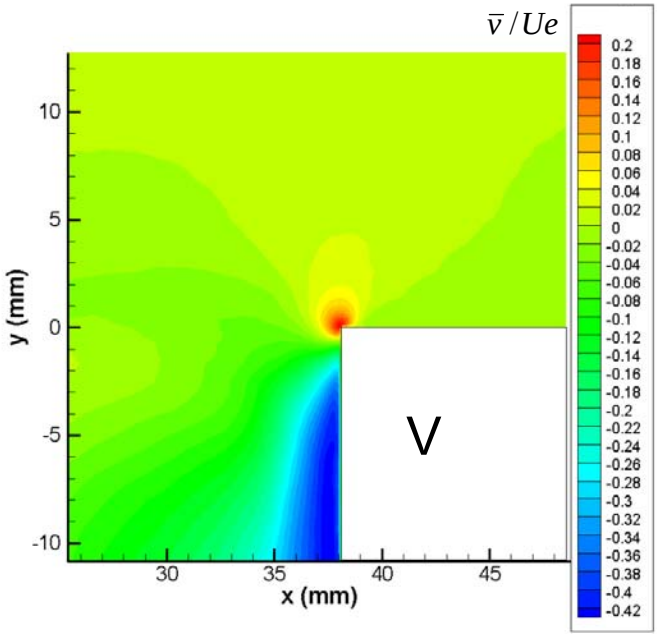

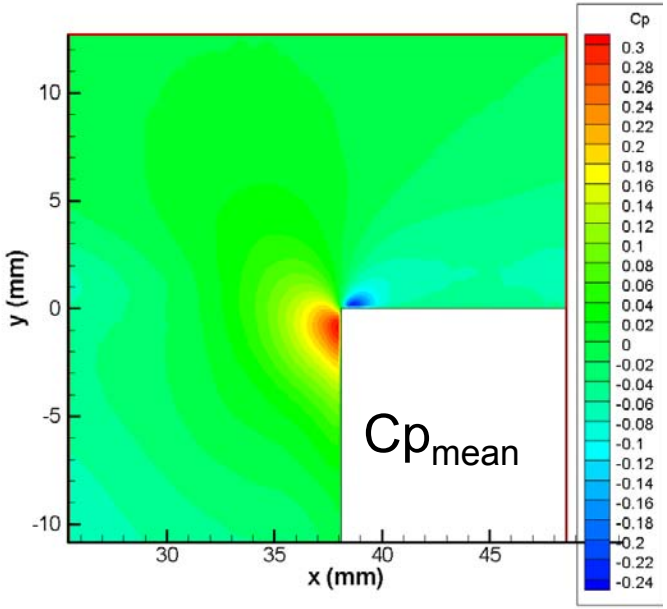

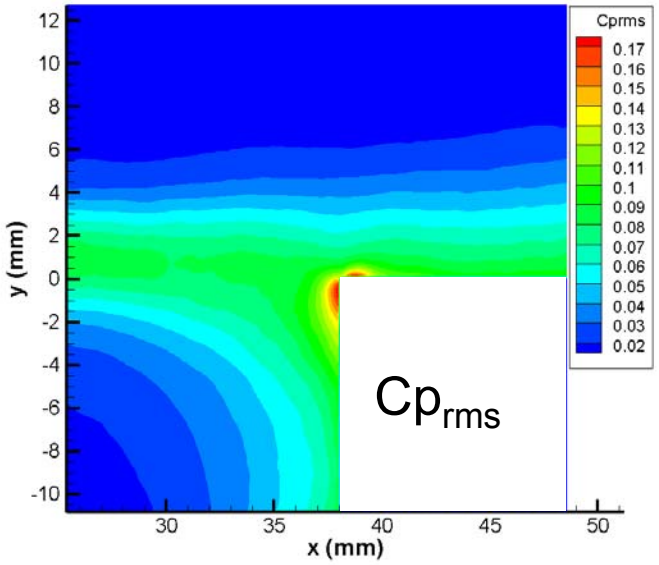

Reynolds Stress Distributions

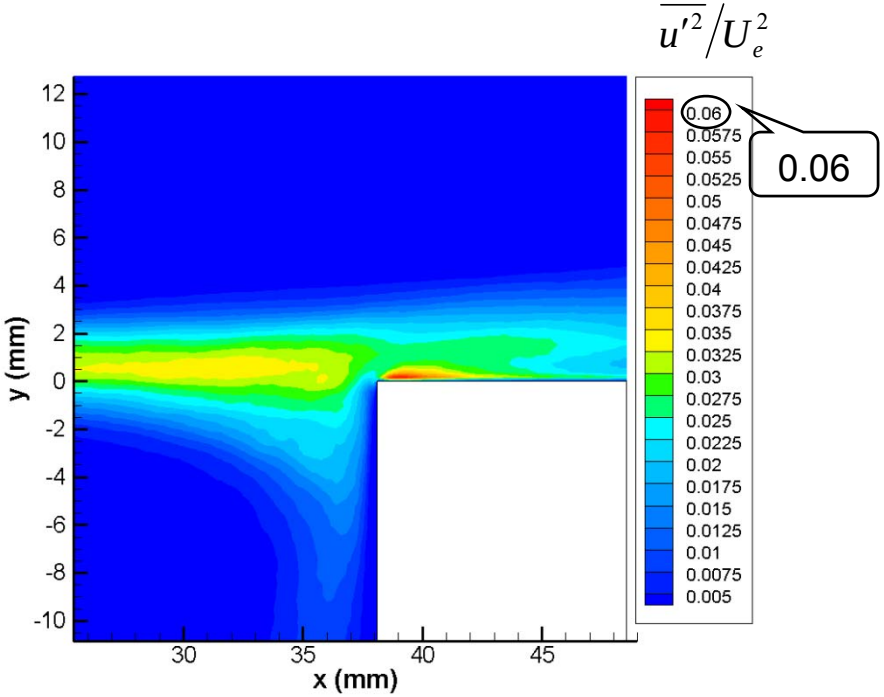

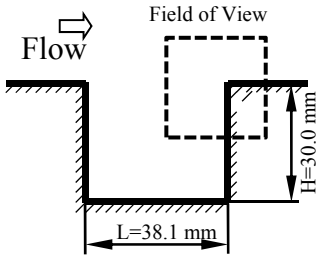

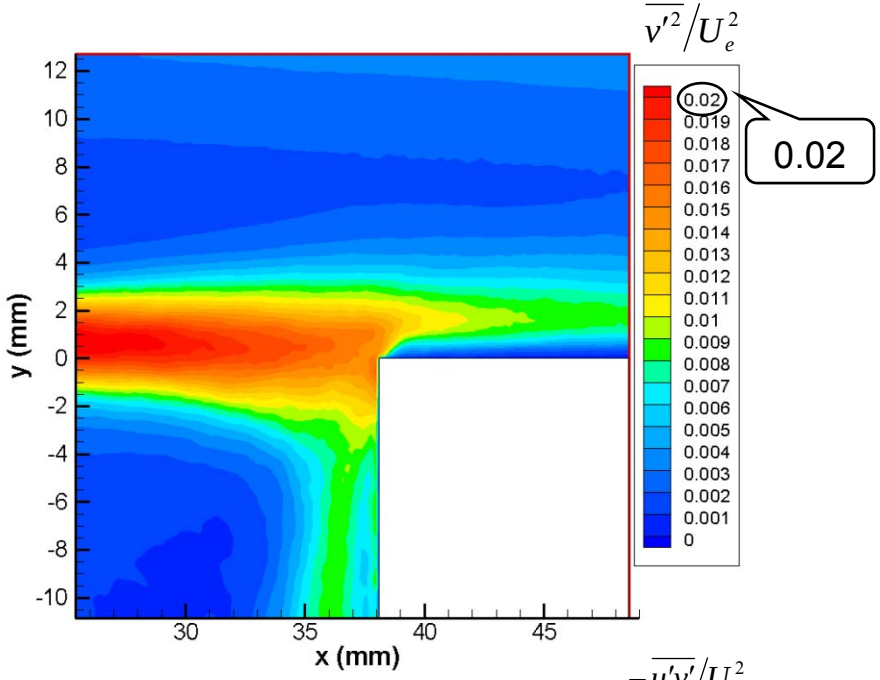

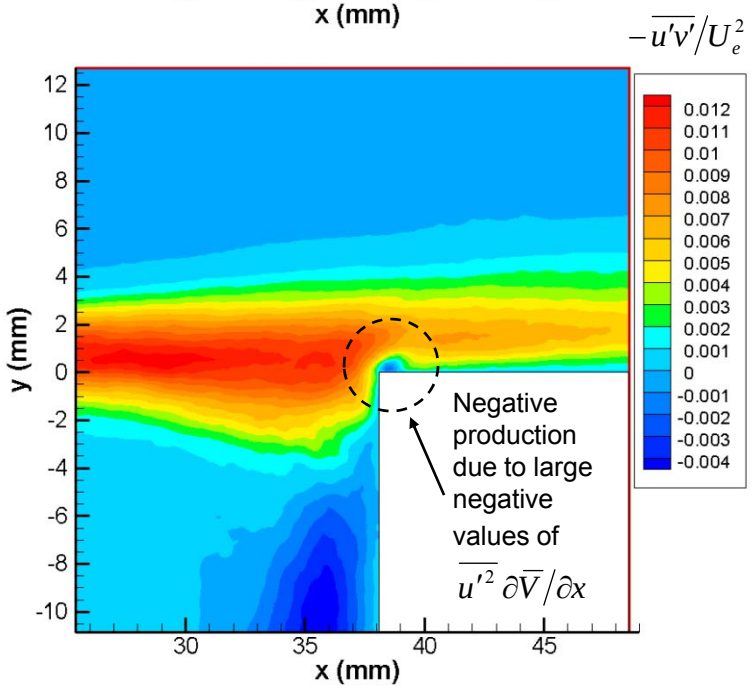

- Other turbulence statistics obtained from measurements (to be shown later on):
  - **Pressure-velocity correlations**;
  - **Pressure-strain correlations**.
- Results of spectrum analysis (Liu and Katz, 2013) are in agreement with theory and our cavitation visualization for this same flow (Liu and Katz, 2008).

The TKE Production

Shear Production

$$-\overline{u'v'}\left(\frac{\partial \overline{U}}{\partial y}+\frac{\partial \overline{V}}{\partial x}\right)\left(L/U_e^3\right)$$

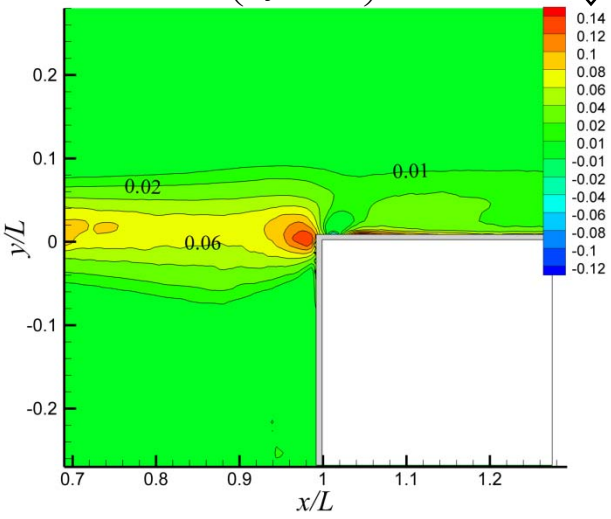

Dilatational Production

$$\left(-\overline{u'^2}\frac{\partial \overline{U}}{\partial x}-\overline{v'^2}\frac{\partial \overline{V}}{\partial y}\right)\left(L/U_e^3\right)$$

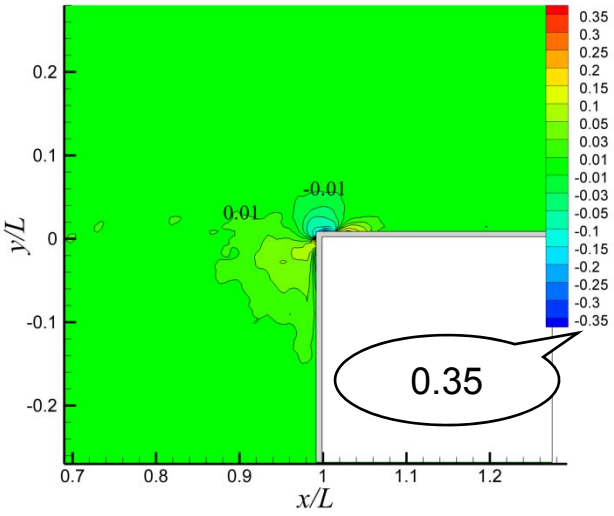

Total In-plane TKE production

$$PL/U_e^3$$

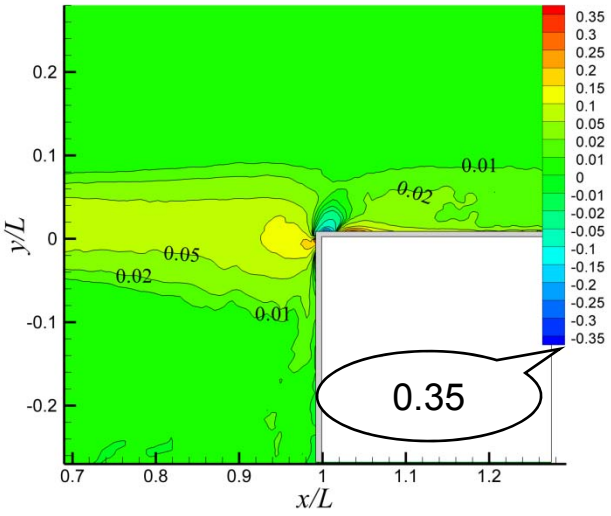

The total In-plane TKE production is defined as:

$$P=-\overline{u'v'}\left(\frac{\partial \overline{u}}{\partial y}+\frac{\partial \overline{v}}{\partial x}\right)+\left(-\overline{u'^2}\frac{\partial \overline{u}}{\partial x}-\overline{v'^2}\frac{\partial \overline{v}}{\partial y}\right)$$

Shear production *Dilatational production*

Conclusion:

- **Production is shear dominated in the shear layer.**
- **Dilatational production becomes significant near the corner.**

Pressure-Velocity Correlation

Ue = **1.2 m/s**; L=38.1mm; Re=**40,000** (based on cavity width); $Re_\lambda = 316$;

Ensemble size: 80,000 data points for 18 seconds.

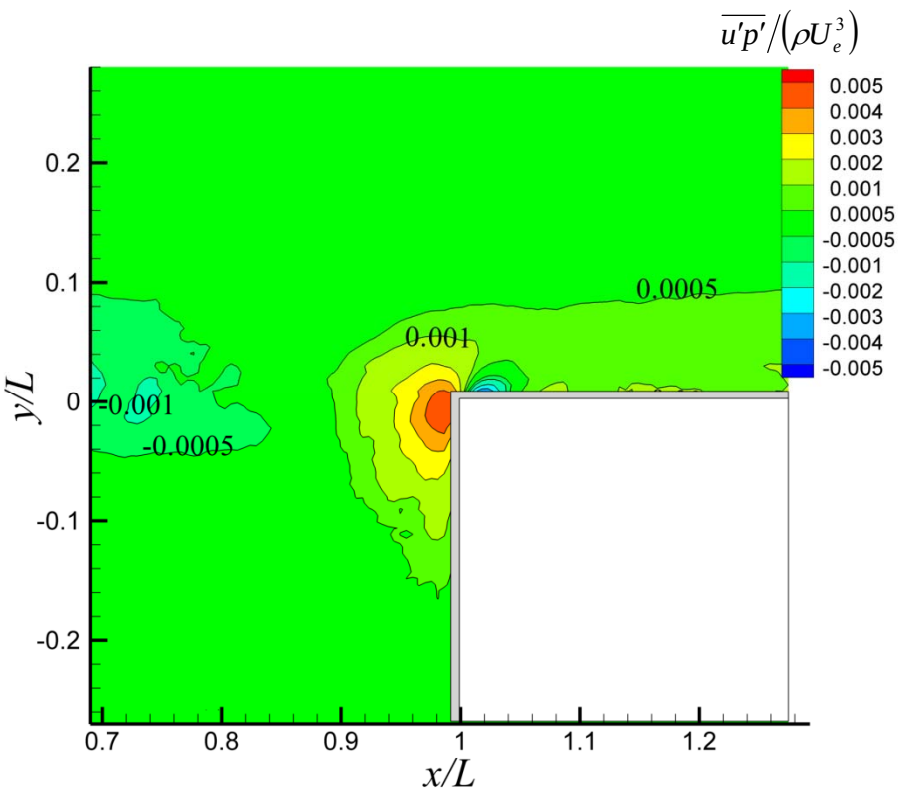

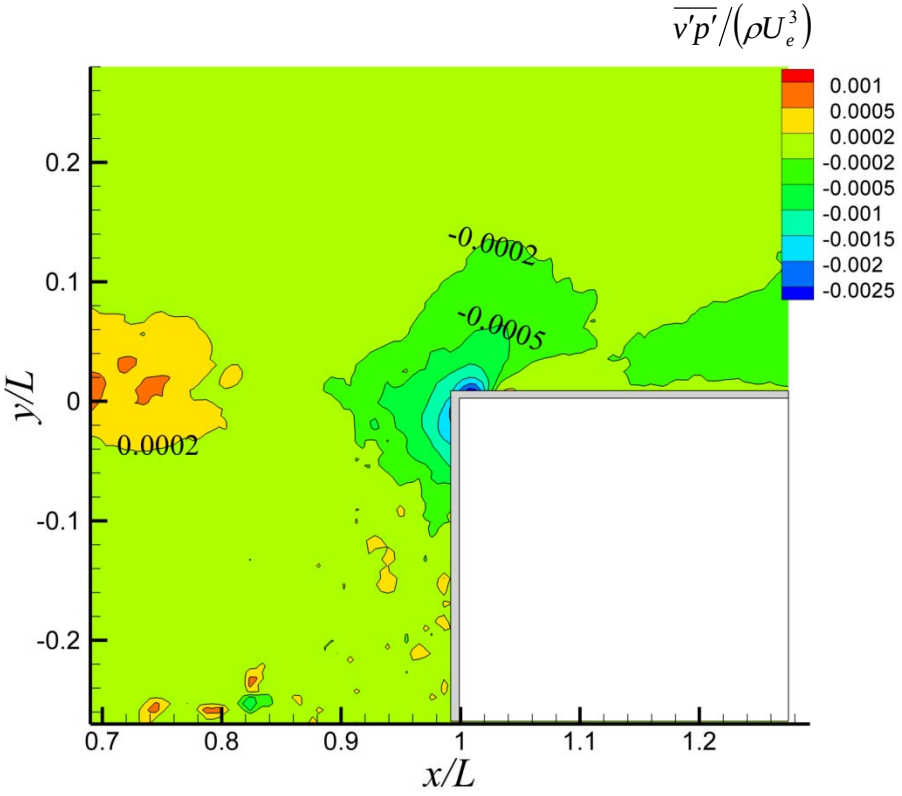

In shear layer:
- **Streamwise acceleration → u increases, p decreases → u′ (+), p′(-) → u′p′(-);**
- **Streamwise deceleration → u decreases, p increases → u′ (-), p′(+) → u′p′(-).**

Impinging on wall:
- **Streamwise acceleration → u increases, p decreases → u′ (+), p′(+) → u′p′(+);**
- **Streamwise deceleration → u decreases, p increases→ u′ (-), p′(-) → u′p′(+).**

Above the wall:
- **High favorable pressure gradient → u′ (+), v′ (+), p′(-) → u′p′(-), v′p′(-);**
- **Low favorable pressure gradient → u′ (-), v′ (-), p′(+) → u′p′(-), v′p′(-).**

- **In shear layer, u-p correlation negative; in front of trailing corner, u-p-correlation positive.**

Pressure-Velocity Correlation

Ue = **10.0 m/s**; L=38.1mm; Re=**335,000** (based on cavity width); Re_λ = 340,

Ensemble size: 1,000 data points for 500 seconds

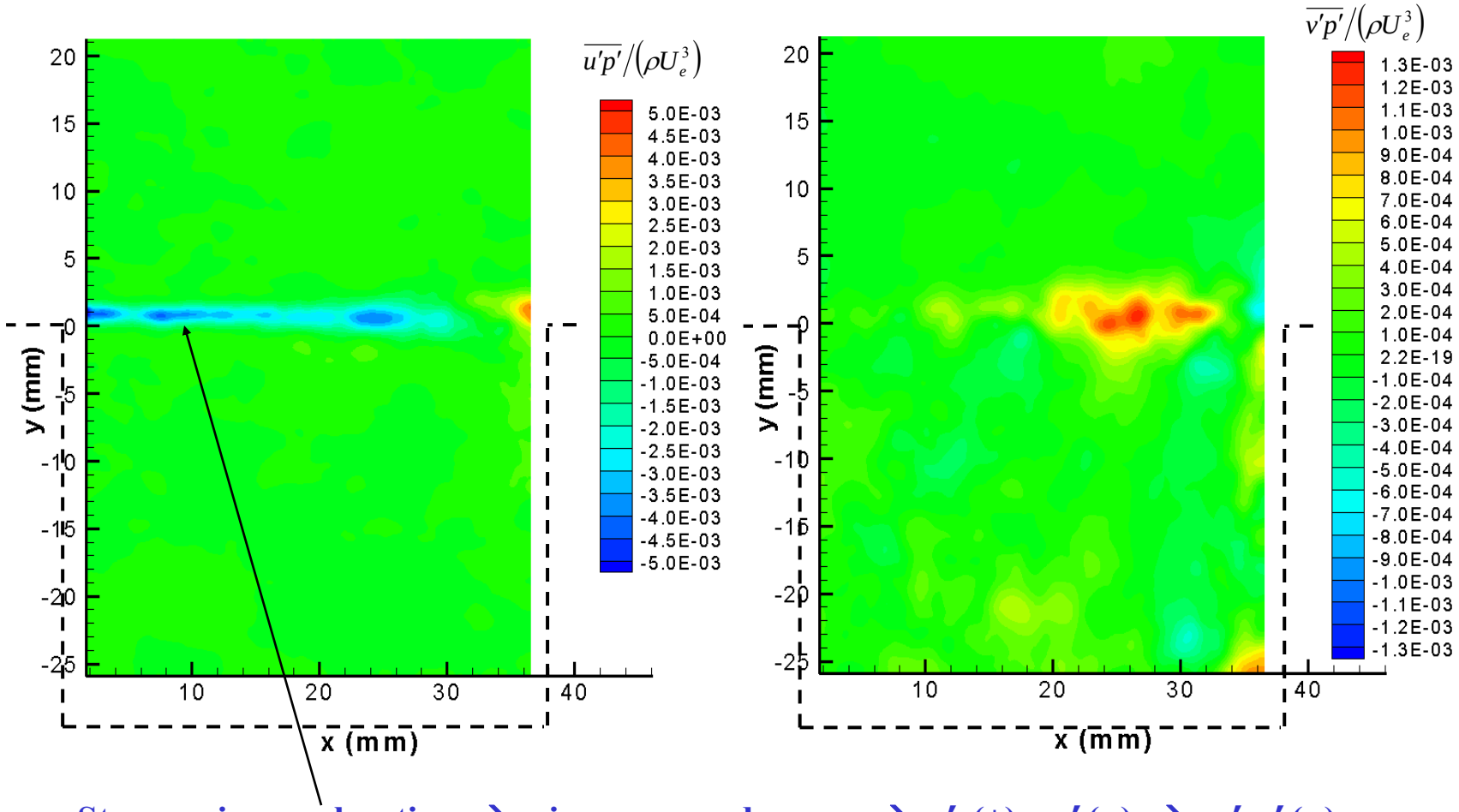

Streamwise acceleration → u increase, p decrease → u′ (+), p′(-) → u′p′(-);
Streamwise deceleration → u decrease, p increase → u′ (-), p′(+) → u′p′(-);

- Hooper and Musgrove (1997) also reported strong negative correlation between fluctuating pressure and streamwise velocity component in a developed pipe flow using a cobra (4-hole) probe.

The u-component Diffusions and the TKE Production

Turbulence diffusion of $\overline{u^2}$

$$\left(-\frac{\partial \overline{u'^3}}{\partial x}-\frac{\partial \overline{u'^2 v'}}{\partial y}\right)\left(L/U_e^3\right)$$

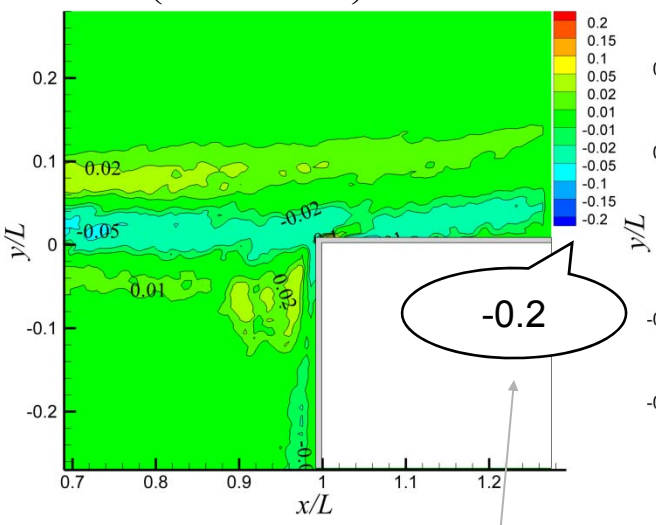

Pressure diffusion of $\overline{u^2}$

$$-\frac{\partial}{\partial x}\left(\frac{2}{\rho}\overline{u'p'}\right)\left(L/U_e^3\right)$$

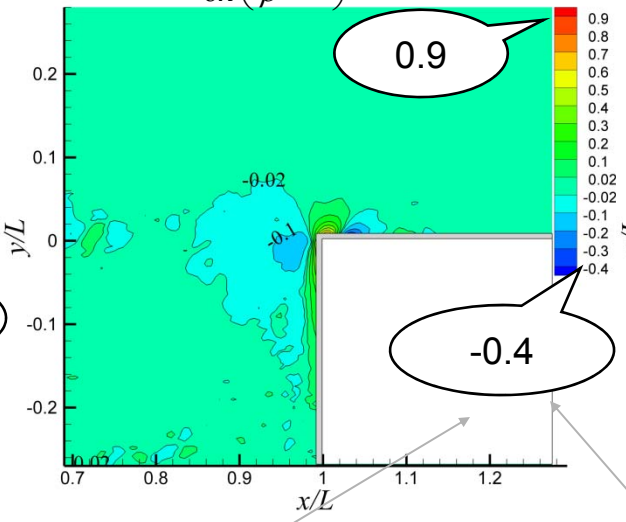

Total In-plane TKE production

$$PL/U_e^3$$

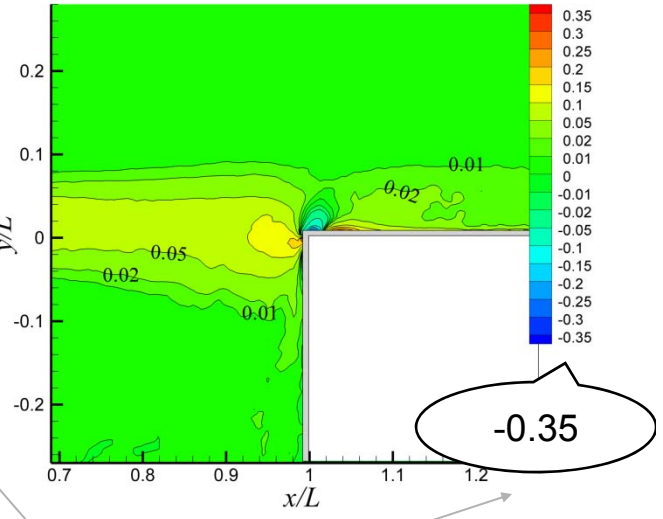

Note: The magnitude of pressure diffusion is of **the same order** as the turbulence diffusion.

The magnitude of the pressure diffusion is **about the same** as the total turbulence kinetic energy (TKE) production.

Conclusion:

- **Turbulence diffusion of u^2 dominates in the shear layer.**
- **Close to the corner, pressure diffusion is significant (thus cannot be neglected in RANS simulation there); away from the corner, pressure diffusion is negligible.**
- **Pressure diffusion term (at least for the u-component) cannot be modeled after the turbulence diffusion since their shape of distribution is different.**
- **Pressure diffusion has similar shape but opposite sign with the production near corner. – A hint for possible modeling relationship.**

The v-component Diffusions and the TKE Production

Turbulence diffusion of $\overline{v^2}$

$$\left(-\frac{\partial \overline{u'v'^2}}{\partial x}-\frac{\partial \overline{v'^3}}{\partial y}\right)\left(L/U_e^3\right)$$

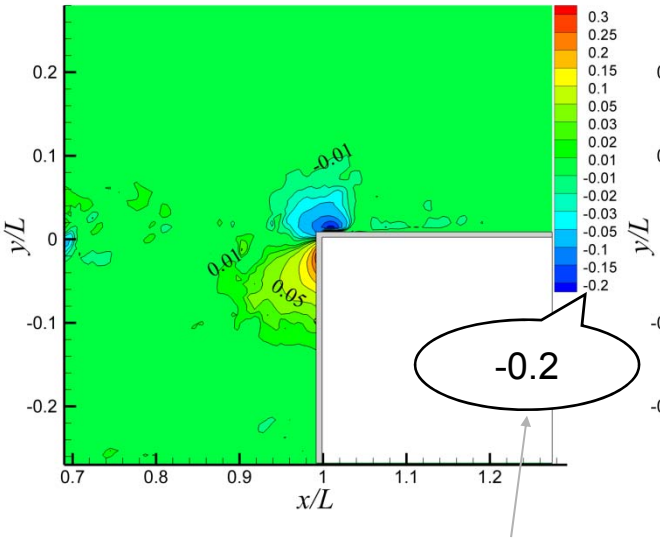

Pressure diffusion of $\overline{v^2}$

$$-\frac{\partial}{\partial y}\left(\frac{2}{\rho}\overline{v'p'}\right)\left(L/U_e^3\right)$$

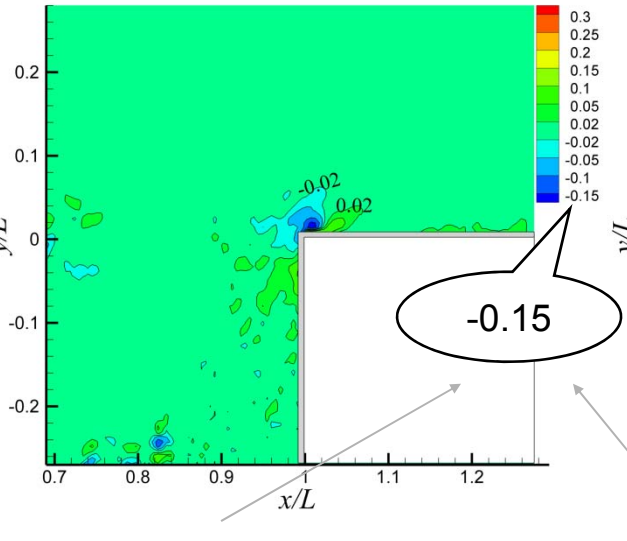

Total In-plane TKE production

$$PL/U_e^3$$

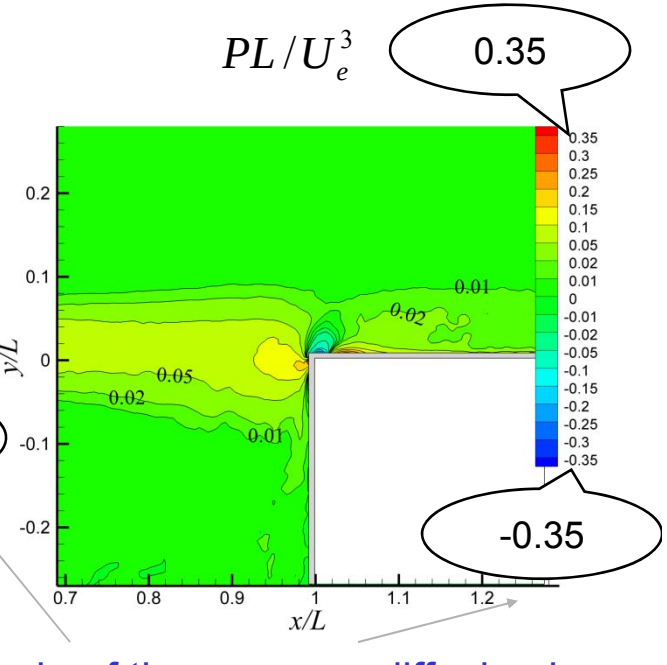

Again, the magnitude of pressure diffusion is **of the same order** as the turbulence diffusion.

The magnitude of the pressure diffusion is **at least comparable** with the total turbulence kinetic energy production.

Conclusion:

- **Turbulence diffusion of u^2 dominates in the shear layer.**
- **Close to the corner, pressure diffusion is significant; away from the corner, pressure diffusion is negligible.**

Remarks on Diffusion Term Modeling

- In the popular eddy viscosity models of RANS (Reynolds-Averaged Navier-Stokes) simulation approach, a common practice is to combine the transport terms and model them as (Chen and Jaw 1998; Pope 2000; Lumley 1978; Fu 1993; Schwarz and Bradshaw 1994):

$$\frac{1}{\rho}\overline{p'u_i'} + \frac{1}{2}\overline{u_i'u_j'u_j'} - 2\nu\overline{u_j's_{ij}'} = -\frac{\nu_T}{\sigma_k}\nabla k$$

  - Knowing the patterns of pressure and turbulence diffusions are fundamentally different, it seems that collectively modelling the diffusion terms all together as shown above may not be justifiable for this turbulent 2-D open cavity shear layer flow.
  - Question : Based on the experimental evidence, can we model the diffusion terms in terms of production in stead of the gradient of *k*?

$$\frac{1}{\rho}\overline{p'u_i'} + \frac{1}{2}\overline{u_i'u_j'u_j'} - 2\nu\overline{u_j's_{ij}'} \propto P_{ij}(?)$$

$$\frac{1}{\rho}\overline{p'u_i'} \propto P_{ij}(?)$$

$$\frac{1}{\rho}\overline{p'u_i'} \propto P_{ij\_dillational}(?)$$

Velocity-pressure-gradient tensor Π_{11} **Pressure-rate-of-strain tensor** R_{11} **Pressure diffusion of** $\overline{u^2}$

$$-\frac{2}{\rho}\overline{u'\frac{\partial p'}{\partial x}}\left(L/U_e^3\right) = \frac{2}{\rho}\overline{p'\frac{\partial u'}{\partial x}}\left(L/U_e^3\right) + -\frac{\partial}{\partial x}\left(\frac{2}{\rho}\overline{u'p'}\right)\left(L/U_e^3\right)$$

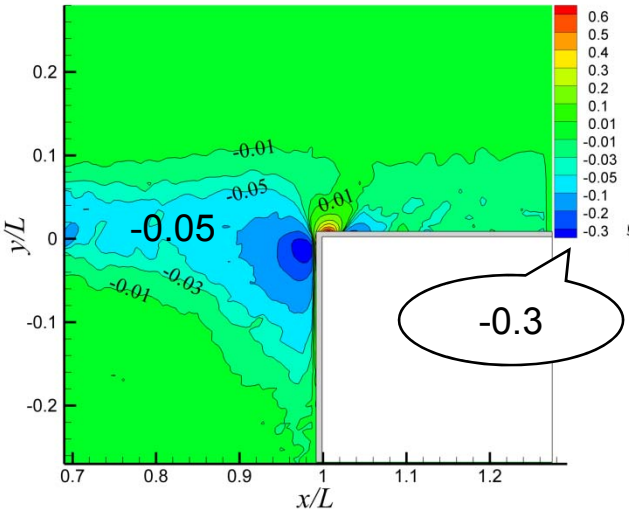

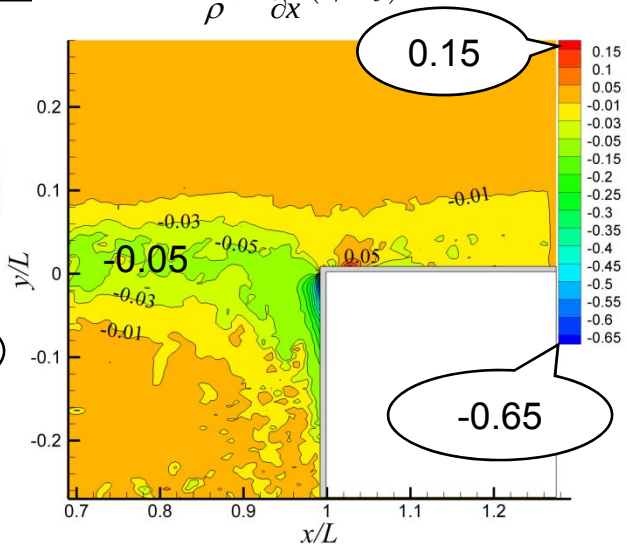

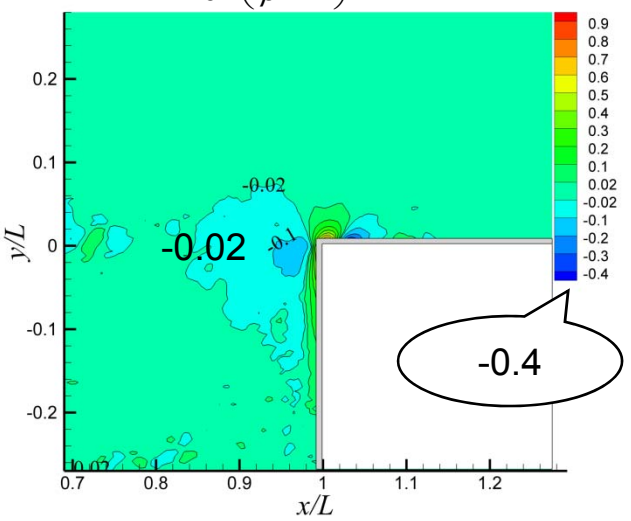

$$\Pi_{11} = R_{11} + D_{11}^{(p)} \qquad \Pi_{22} = R_{22} + D_{22}^{(p)}$$

Ue = 1.25 m/s; Re=40,000

Velocity-pressure-gradient tensor Π_{22} **Pressure-rate-of-strain tensor** R_{22} **Pressure diffusion of** $\overline{v^2}$

$$-\frac{2}{\rho}\overline{v'\frac{\partial p'}{\partial y}}\left(L/U_e^3\right) = \frac{2}{\rho}\overline{p'\frac{\partial v'}{\partial y}}\left(L/U_e^3\right) + -\frac{\partial}{\partial y}\left(\frac{2}{\rho}\overline{v'p'}\right)\left(L/U_e^3\right)$$

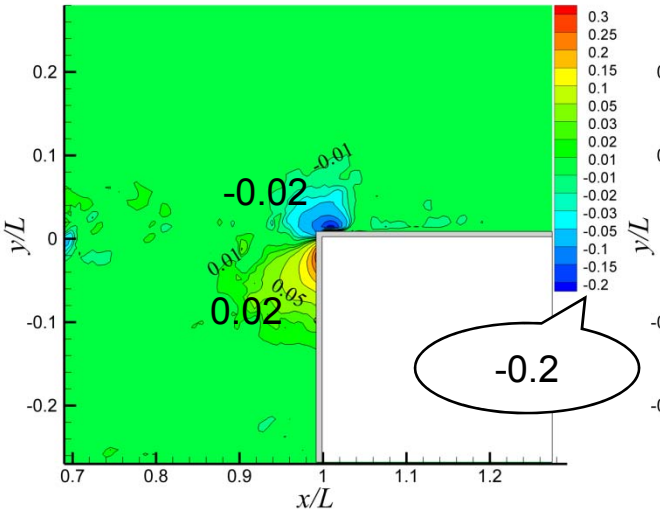

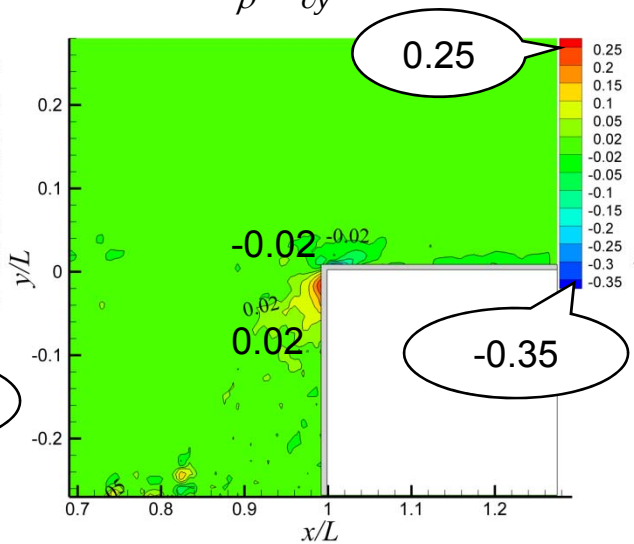

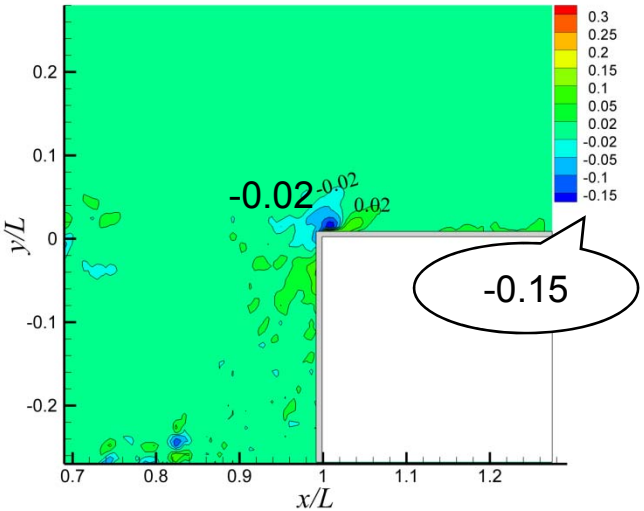

Reynolds Stress Distributions

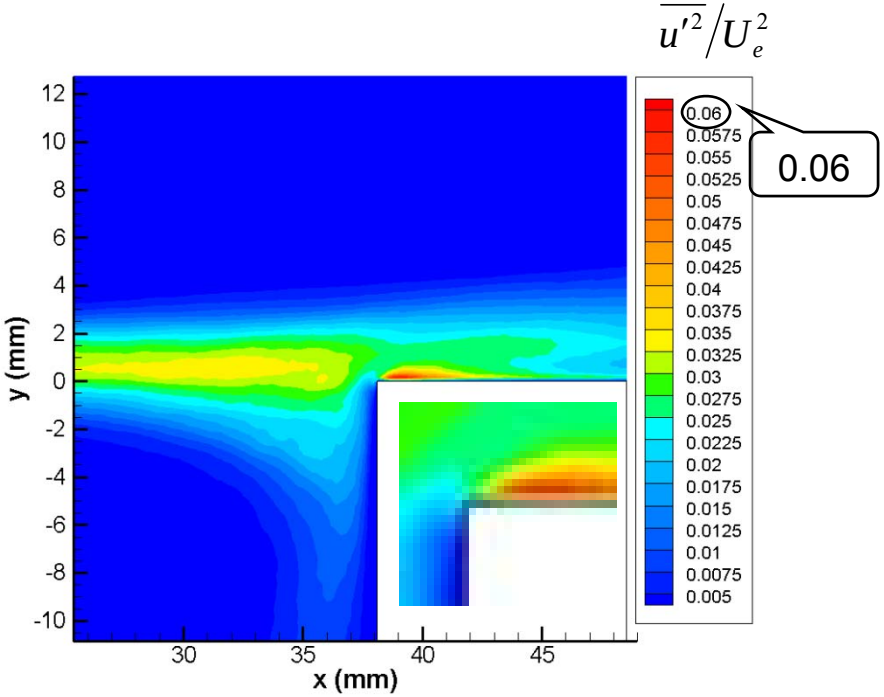

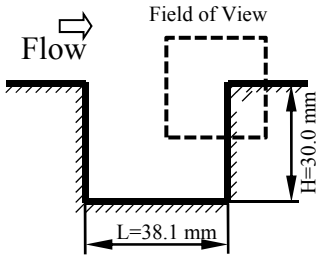

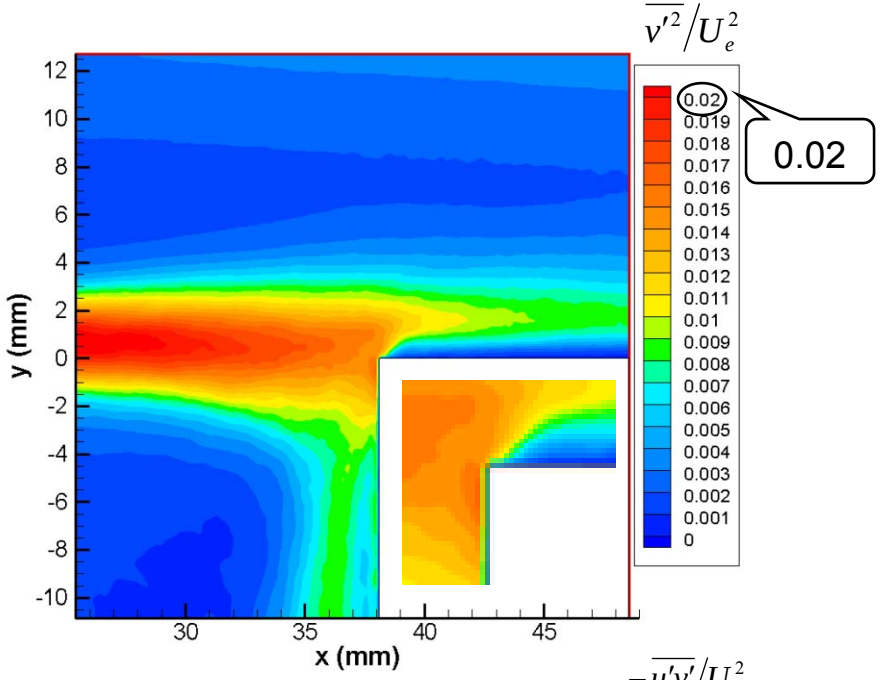

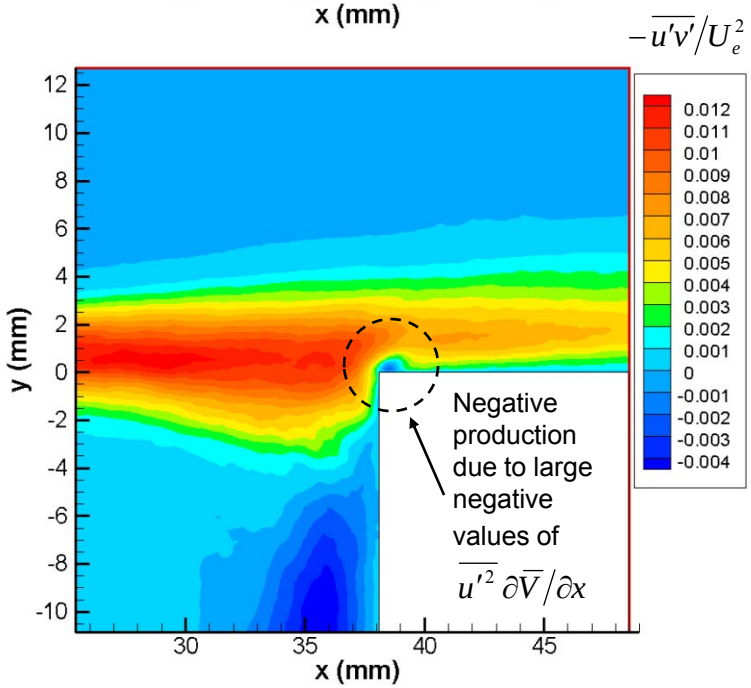

- Other turbulence statistics obtained from measurements (to be shown later on):
  - **Pressure-velocity correlations**;
  - **Pressure-strain correlations**.
- Results of spectrum analysis (Liu and Katz, 2013) are in agreement with theory and our cavitation visualization for this same flow (Liu and Katz, 2008).

Observations

- **Pressure and velocity correlation:**
  - **p' and u'** are negatively correlated in most of the shear layer. However, close to the cavity trailing corner, the p-u correlation gradually decreases in magnitude, and eventually changes its sign, creating a positive peak just upstream of the trailing edge, followed by a negative correlation again above the trailing corner.
  - **p' and v'** are positively correlated in most of the shear layer, and become negatively correlated in the area surrounding the cavity trailing corner.
- **Diffusion:**
  - In the shear layer, the u-component turbulence diffusion dominates.
  - Close to the corner, pressure diffusion is significant, and its magnitude is on the same order as those of the turbulence diffusion and the total in-plane turbulence production.
  - The distribution patterns of the turbulence diffusion and the pressure diffusion are considerably different.

Observations (continued)

- **Diffusion (continued):**
  - The u- and the v-component pressure diffusion terms have opposite signs at corresponding locations surrounding the trailing corner of the cavity, where the peaks of the v-component pressure diffusion are smaller in magnitude than those of the u-component counterparts.
- **Velocity-pressure-gradient tensor and pressure-strain:**
  - In the shear layer, the u-component velocity-pressure-gradient tensor Π_{11} and the pressure-strain R_{11} have dominant values in comparison with their v-component counterparts.
  - The pressure-strain term R_{11} keeps a strong negative value throughout the shear layer, peaking at the impingement point on the trailing wall of the cavity.
  - The pressure-strain term R_{22} has a weak positive value in the shear layer.
  - The intercomponent fluctuation energy transfer completely changes its scheme on top of the trailing corner, where R_{11} takes a positive value and R_{22} a negative one.
  - Considering the negative turbulence production there, the pressure-strain intercomponent energy transfer is the major mechanism that is responsible for the high u-component fluctuation energy (and also the low v-component fluctuation energy) occurring on top of the trailing corner of the open cavity.

Concluding Remarks

- **Pressure diffusion and turbulence diffusion follow different patterns**. Collectively modelling the pressure diffusion terms with other diffusion terms may not be justifiable for the turbulent 2-D open cavity shear layer flow.
- **Pressure gradient plays a critical role in defining the picture of turbulence transport**. Both the pressure diffusion and the pressure strain terms are intensified at places (e.g., impingement or re-attachment regions) of high pressure gradients. The change in pressure gradient results in the change in both the pressure diffusion and pressure strain terms.
- **The pressure-related terms have substantial impact on the dynamics of turbulence transport throughout the shear layer**.
- **Lack of data, especially high quality, right type of data, hinders the development of turbulence modeling in the past 20 years. The relationships between the pressure-related terms and other transport terms are far from being exhausted. Thus more explorations are needed and legitimate**.
- The complicated intercomponent energy transfer process clearly shows the **challenges (and perhaps opportunities)** that turbulence modeling faces in turbulent cavity shear layer flow in particular, and perhaps separation and reattachment flow in general.

Acknowledgments

- The research was sponsored in part by
  - the **Office of Naval Research** (Ki-Han Kim and Debbie Nalchajian are the Program Officers),
  - and in part by **National Science Foundation** grant CBET-1438203 (R. Joslin is the Program Director).
  - The financial support from the UGP program of the **San Diego State University** is also gratefully acknowledged.

- Most of the content of this talk can be found in
  - Liu, X. and Katz, J., Pressure rate of strain, pressure diffusion and velocity pressure gradient tensor measurements in a cavity shear layer flow, 55th AIAA Aerospace Sciences Meeting, AIAA SciTech Forum, (**AIAA 2017-1478**), http://dx.doi.org/10.2514/6.2017-1478.
  - Also submitted to *AIAA Journal* for review.

- Other information:
  - Google keyword: Pressure PIV.
  - SDSU Lab website: http://liu.sdsu.edu
  - Email: Xiaofeng.Liu@mail.sdsu.edu